In the present study, we observed COX-2 expression during focal brain ischemia in a primate thromboembolic stroke model in which regional CBF and CMRglc were evaluated using high-resolution PET scanning. In this model, a reduction was observed in CBF in the ischemic temporal cortex and basal ganglia to <40% of the CBF in the contralateral hemisphere 1 h following embolization, while CBF in the ischemic parietal cortex was found to be >40% of contralateral values; these results support previous findings [7,8]. The flow threshold for infarct development was 12–15 ml $100g^{-1}$ min^{-1} (40% of contralateral values) in this model [8].

Our finding of an increase in COX-2 mRNA expression following focal brain ischemia that was demonstrable in the hemisphere ipsilateral to the arterial embolization, was consistent with previous findings in rodent models [1,9,10]. In the ischemic core in which a significant decrease in CBF were accompanied by reduced CMRglc, the upregulation in COX-2 mRNA expression that was seen following 2 h of ischemia decreased by 24 h of ischemia. The disappearance of COX-2 following 24 h of ischemia paralleled the reduction in expression of mRNA for the house-keeping gene, GAPDH, which indicated that ischemic injury was already apparent at this time in the basal ganglia as well as in the temporal cortex, a finding that is consistent with our previous report [8]. On the other hand, in the peri-infarct area, induced expression of COX-2 mRNA was still present following 24 h of ischemia in the parietal cortex, as was a mild CBF reduction, though CMRglc was maintained. Delayed induction of COX-2 in the infarcted human brain was suggested to promote reconstitutive processes in the form of tissue scarring and remodeling of the surviving neural networks [11]. Although interpretation of the results in this study should be careful because of the limited number of primates, we propose that the regulation of COX-2 expression is different in the ischemic core than in the peri-infarct area, and that therefore the role of COX-2 in focal ischemic tissues is determined by the depth and duration of CBF reduction.

Acknowledgements

We are grateful to Dr Takeo Abumiya for his suggestions concerning the preparation of this manuscript, and thank Mr. Norimasa Ejima and Miss Yumi Miyamoto for their technical assistance. This work was supported in part by Special Coordination Funds for Promoting Science and Technology (Strategic Promotion System for Brain Science) from the Ministry of Education, Culture, Sports, Science and Technology of Japan, by a Grant-in-Aid for Scientific Research from the Japan Society for the Promotion of Science, by a Grant from Japan Heart Foundation Research, by a Grant from the Takeda Medical Research Foundation in Japan, and by Research Grants for Cardiovascular Diseases (11C-3, 12A-2) from the Ministry of Health, Labor and Welfare of Japan.

References

[1] Y. Collaco-Moraes, B. Aspey, M. Harrison, J.D. Belleroche, Cyclo-oxygenase-2 messenger RNA induction in focal cerebral ischemia, J. Cereb. Blood Flow Metab. 16 (1996) 1366–1372.
[2] W.-D. Heiss, R. Graf, K. Wienhard, L.R. Saito, T. Fujita, G. Rosner, R. Wagner, Dynamic penumbra demonstrated by sequential multitracer PET after middle cerebral artery occlusion in cats, J. Cereb. Blood Flow Metab. 14 (1994) 892–902.
[3] C. Iadecola, C. Forster, S. Nogawa, H.B. Clark, M.E. Ross, Cyclooxygenase-2 immunoreactivity in the human brain following cerebral ischemia, Acta. Neuropathol. 98 (1999) 9–14.
[4] C. Iadecola, K. Niwa, S. Nogawa, X. Zhao, M. Nagayama, E. Araki, S. Morham, M.E. Ross, Reduced susceptibility to ischemic brain injury and *N*-methyl-D-aspartate-mediated neurotoxicity in cyclooxygenase-2-deficient mice, Proc. Natl. Acad. Sci. USA 98 (2001) 1294–1299.
[5] H. Inoue, T. Tanabe, K. Umesono, Feedback control of cyclooxygenase-2 expression through PPARgammma, J. Biol. Chem. 275 (2000) 28028–28032.
[6] H. Inoue, C. Yokoyama, S. Hara, Y. Tone, T. Tanabe, Transcriptional regulation of human prostaglandin-endoperoxide synthase-2 gene by lipopolysaccharide and phorbol ester in vascular endothelial cells, J. Biol. Chem. 270 (1995) 24965–24971.
[7] G. Kito, A. Nishimura, T. Susumu, R. Nagata, Y. Kuge, C. Yokota, K. Minematstu, Experimental thromboembolic stroke in cynomolgus monkey, J. Neurosci. Methods 105 (2001) 45–53.
[8] Y. Kuge, C. Yokota, M. Tagaya, Y. Hasegawa, A. Nishimura, G. Kito, N. Tamaki, N. Hashimoto, T. Yamaguchi, K. Minematsu, Serial changes in cerebral blood flow and flow-metabolism uncoupling in primates with acute thromboembolic stroke, J. Cereb. Blood Flow Metab. 21 (2001) 202–210.
[9] S. Miettinen, F.R. Fusco, J. Yrjanheikki, R. Keinanen, T. Hirvonen, R. Roivainen, M. Narhi, T. Hokfelt, J. Koistinaho, Spreading depression and focal brain ischemia induce cyclooxygenase-2 in cortical neurons through *N*-methyl-D-aspartic acid-receptors and phospholipase A2, Proc. Natl. Acad. Sci. USA 94 (1997) 6500–6505.
[10] S. Nogawa, F. Zhang, M.E. Ross, C. Iadecola, Cyclo-oxygenase-2 gene expression in neurons contributes to ischemic brain damage, J. Neurosci. 17 (1997) 2746–2755.
[11] T. Sairanen, A. Ristimaki, M.-L. Karjalainen-Lindsberg, A. Paetau, M. Kaste, P.J. Lindsberg, Cyclooxygenase-2 induced globally in infarcted human brain, Ann. Neurol. 43 (1998) 738–747.
[12] K. Wienhard, M. Dahlbom, L. Eriksson, C. Michel, T. Bruckbauer, U. Pietrzyk, W.D. Heiss, The ECAT EXACT HR: performance of a new high resolution positron scanner, J. Comput. Assist. Tomogr. 18 (1994) 110–118.
[13] K. Yamagata, K.I. Andreasson, W.E. Kaufmann, C.A. Barnes, P.F. Worley, Expression of a mitogen-inducible cyclooxygenase in brain neurons: regulation by synaptic activity and glucocorticoids, Neuron 11 (1993) 371–386.

Journal of Cerebral Blood Flow & Metabolism
23:395–398 © 2003 The International Society for Cerebral Blood Flow and Metabolism
Published by Lippincott Williams & Wilkins, Inc., Philadelphia

Short Communication

Cyclooxygenase-2 Expression Associated With Spreading Depression in a Primate Model

*Chiaki Yokota, †Hiroyasu Inoue, ‡Yuji Kuge, §Takeo Abumiya, ‖Masafumi Tagaya, ¶Yasuhiro Hasegawa, #Norimasa Ejima, **Nagara Tamaki, and ¶Kazuo Minematsu

**Cerebrovascular Laboratory, Department of Pathogenesis, and †Department of Pharmacology, National Cardiovascular Center Research Institute, Departments of ‡Tracer Kinetics and **Nuclear Medicine, Graduate School of Medicine, Hokkaido University §Department of Neurosurgery, Ebetu Hospital, ‖Department of Medicine, National Osaka Hospital, ¶Cerebrovascular Division, Department of Medicine, National Cardiovascular Center, and #Institute for Biofunctional Research Co., Inc., Osaka, Japan*

Summary: The authors previously provided evidence that spreading depression (SD) can be evoked in primates. Cyclooxygenase-2 (COX-2) expression has been found to increase in the rodent cortex undergoing SD, and the authors sought to determine whether this association exists in primate brain. In the present study, neuronal COX-2 expression was induced during SD in the primate cortex. The mean expression ratio of COX-2 messenger RNA in animals with SD was significantly higher than that measured in controls (1.69 vs. 0.5; $P = 0.02$). Induction of COX-2 in these animals was also detected by human microarray analysis. Results show that, as in rodents, neuronal COX-2 is induced in the primate cortex in response to SD. **Key Words:** Spreading depression—Cyclooxygenase-2—Microarray analysis—Primate.

Cortical spreading depression (SD), the reversible depression of cortical electrical activity, plays a role in the development of cerebral ischemic injury and migraine (Lauritzen et al., 1983; Olesen et al., 1981; Woods et al., 1994). Repetitive, pathologic SDs were similarly found to play a role in the development of ischemic injury under conditions of focal brain ischemia in rats (Gill et al., 1992; Hossmann, 1994; Iijima et al., 1992; Takano et al., 1996). Changes in cerebral blood flow (CBF) in experimental SD models in rats and cats were characterized by transient focal cortical hyperemia, followed by persistent hypoperfusion (Kuge et al., 2000; Lauritzen et al., 1982; Piper et al., 1991). Recently, we provided the first direct evidence that SD, accompanied by focal cortical hyperemia, can be evoked in primates (Yokota et al., 2002). The long-lasting hypoperfusion that followed this hyperemia in rats and cats has not been observed in primates.

The gene for cyclooxygenase-2 (COX-2), a rate-limiting enzyme in prostaglandin synthesis, was induced in the nonprimate cortex during SD (Koistinaho et al., 1999; Miettinen et al., 1997). Cyclooxygenase-2 appeared to mediate the increase in CBF produced by synaptic activity in the somatosensory cortex in mice (Niwa et al., 2000). The contribution of SD and its associated genes to the pathogenesis of human brain diseases has not been elucidated.

As a first step in determining which genes show altered expression during SD in primates, we examined whether the COX-2 gene was upregulated. Using a human complementary DNA (cDNA) array system, we also examined the effect of SDs on gene-expression profiles.

MATERIALS AND METHODS

Spreading depression model and brain preparation

Nine adult, male cynomolgus monkeys were divided into two groups: a normal control group (group C, n = 3) and a group in which SD was evoked by applying 3.3-mol/L KCl to

Received September 18, 2002; final version received December 9, 2002; accepted December 9, 2002.

This study was supported in part by Special Coordination Funds for Promoting Science and Technology (Strategic Promotion System for Brain Science) from the Ministry of Education, Culture, Sports, Science and Technology of Japan, by a Grant-in-Aid for Scientific Research from the Japan Society for the Promotion of Science, by a grant from the Takeda Medical Research Foundation in Japan, and by a Japan Heart Foundation Research Grant.

Address correspondence and requests to Dr. Yokota, Cerebrovascular Laboratory, National Cardiovascular Center Research Institute, 5–7-1 Fujishirodai, Suita, Osaka 565-8565, Japan; e-mail: cyokota@ri.ncvc.go.jp

DOI: 10.1097/01.WCB.0000055293.67563.2E

the cortex (group SD, n = 6). All procedures were approved by our Institutional Animal Research Committee and were performed in accordance with standards published by the National Research Council in the *Guide for the Care and Use of Laboratory Animals.*

Shifts of direct current potential were measured in four animals in the SD group only with a microelectrode placed just rostral to the chemical stimulation site; a single episode was recorded in three animals, and six episodes were recorded in one animal. Direct current potential was measured in the remaining two animals with a microelectrode that was placed caudal to the chemical stimulation site as well as with microelectrodes placed rostral to the chemical stimulation site; one of these animals was subjected to eight recording episodes at this site, whereas the remaining animal was subjected to two direct current shifts, each of which was recorded from a point that was rostrally adjacent to the chemical stimulation site, as well as to six episodes at the caudal site.

Two hours after KCl application, the brains from these animals were perfused with cold saline, after which the animals were killed and the brains removed. Several samples from each cortex were harvested and stored at −80°C until use, whereas other samples were embedded in paraffin.

RNA blot analysis

RNA preparation and blot analysis were performed as previously described (Inoue et al., 1995). Cyclooxygenase-2 messenger RNA (mRNA) in each region was expressed as the ratio of the COX-2 mRNA signal to the GAPDH mRNA signal in that region (expression ratio).

Microarray analysis

Microarray analysis was conducted using Genome System (St. Louis, MO, U.S.A.) as described elsewhere (Lyer et al., 1999). The microarray contained 9,182 elements: 8,412 unique annotated genes or expressed sequence tags, and 4,757 characterized human protein genes. Left cortical RNAs from the SD (>5 episodes; n = 3) and control (n = 3) groups were pooled. Poly $(A)^+$ RNAs were purified from these RNAs using oligo$(dT)_{30}$-latex (Takara, Inc., Shiga, Japan) to use as templates for cDNA synthesis. The cDNA probes were reverse transcribed with 5'Cy3 or fluorescently labeled Cy5 and were hybridized with Human UniGEM V (version 2.0). The average of the total Cy3 and Cy5 signals yielded a ratio that was used to normalize the signals.

Immunoblot analyses

Left temporal cortical samples were weighed and homogenized in 10 volumes of cold 62.5-mmol/L Tris buffer (pH 6.8) containing 1% sodium dodecylsulfate, 10% glycerin, and 5% 2-mercaptoethanol. Tissue homogenates were heated to 90°C for 5 minutes and then centrifuged at 15,000*g* for 10 minutes at 4°C. The supernatants were separated by SDS-PAGE (5% to 20% acrylamide gradient) and proteins transferred onto a nitrocellulose sheet. The blots were incubated with anti–COX-2 antibody (dilution 1:1,000; Cayman Chemical, Ann Arbor, MI, U.S.A.) for 1 h at 25°C and were then washed in 50-mmol/L phosphate-buffered saline (pH 7.4) containing 0.05% Tween 20.

Immunohistochemistry

A mirror-sectioning technique was used to colocalize COX-2 and microtubule-associated protein 2 (MAP-2), a neuronal skeletal protein. Deparaffinized temporal cortical sections (3 μm) were incubated with a polyclonal anti–COX-2 antibody (dilution 1:100; Cayman Chemical) and a monoclonal anti–MAP-2 antibody (clone HM-2; dilution 1:2,400; Sigma, St. Louis, MO, U.S.A.) overnight at 4°C. The sections were washed with phosphate-buffered saline, and biotinylated goat anti–rabbit immunoglobulin (Vector Laboratories, Burlingame, CA, U.S.A.) or biotinylated $F(ab')_2$ rabbit anti–mouse immunoglobulin (dilution 1:500; Dako, Carpinteria, CA, U.S.A.) was applied to the sections, which were then incubated for 30 minutes at 25°C. Labeling was visualized using a Vectastain Elite Kit (Vector Laboratories).

Statistical analysis

Data are expressed as the mean ± standard deviation. Comparisons of COX-2 mRNA expression between groups were made using the Mann-Whitney *U* test. A two-tailed *P* value less than 0.05 was considered to be significant.

RESULTS

Expression of cyclooxygenase-2 mRNA

Cyclooxygenase-2 mRNA expression increased in the cortex in which SD was induced (left) compared with both the contralateral side and the left cortex in group C (Fig. 1A). The expression ratio of COX-2 mRNA in the left cortex in the SD group (1.69 ± 0.57) was significantly greater ($P = 0.02$) than in the left cortex in group C (0.5 ± 0.05; Fig. 1B).

Cyclooxygenase-2 localization

Immunoblots revealed a 70- to 72-kd COX-2–immunoreactive band (Gidlund et al., 1981) in tissue derived from the SD group, which was barely detectable in group C (Fig. 1C). Immunoreactive neurons were observed in animals that received six SD episodes rostral to the chemical stimulation site (Fig. 1D). Immunoreactive MAP-2 was demonstrable in the same neurons that displayed COX-2 immunoreactivity.

Gene-expression patterns

Increases in normalized gene-expression signals above 1.5-fold were observed for two genes among a total 9,182 elements: the COX-2 (1.6-fold) and basic transcription element–binding protein 1 (1.6-fold) genes. Twenty-one elements were found to be different by at least 1.4-fold. Figure 2 shows representative images of scanned arrays hybridized with left cortical samples.

DISCUSSION

Previous studies have suggested that COX-2 plays a role in the development of ischemic injury during focal brain ischemia in rodents (Collaco-Moraes et al., 1996;

FIG. 2. Gene-expression patterns in the brains of animals in the spreading depression (SD) and control (C) groups. Representative images of scanned arrays hybridized with cortical samples from C and SD animals are shown. Of the 9,182 elements that were examined, expression of the cyclooxygenase-2 gene (red circles) was found to be increased by 1.6-fold in the SD group.

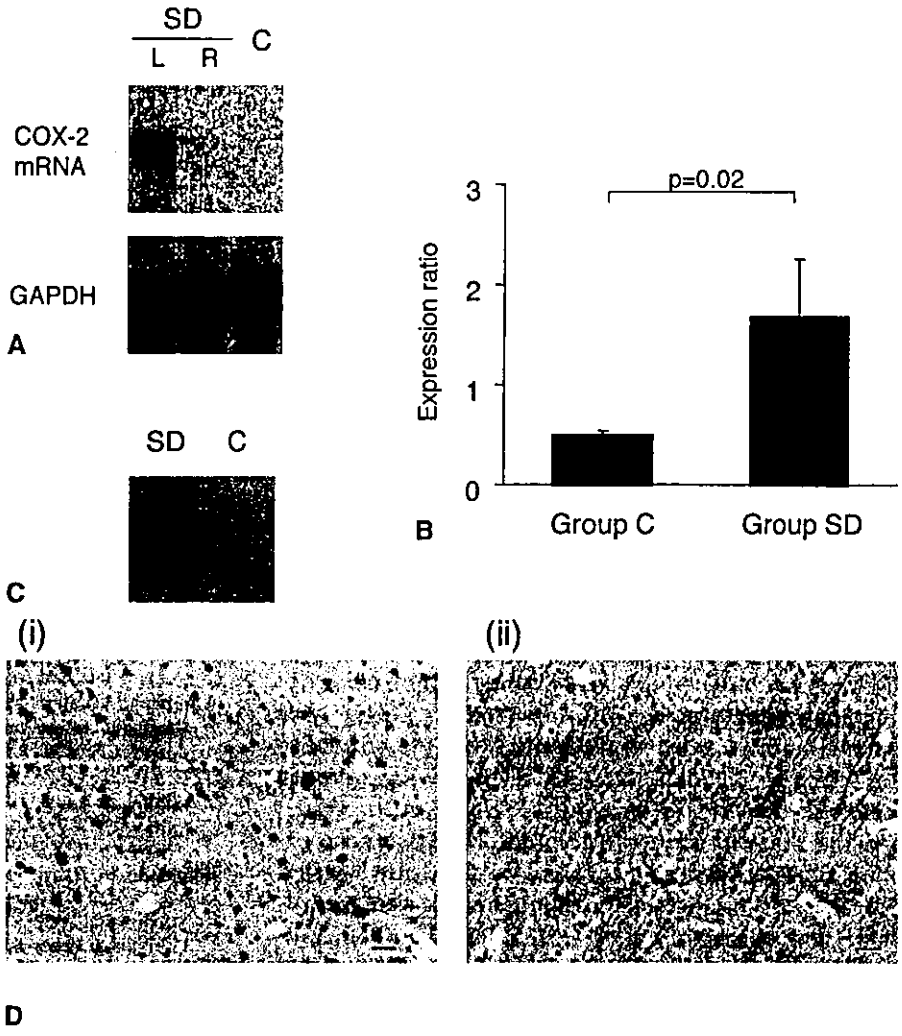

FIG. 1. Cyclooxygenase-2 (COX-2) expression in the primate brain. **(A)** Autoradiograms of COX-2 (top) and glyceraldehyde-3-phosphate dehydrogenase (GAPDH) messenger RNA (bottom) from normal (group C) and spreading depression (SD) animals (group SD). Note that induced COX-2 expression was prominent in the left cortical samples (ipsilateral to the side in which SD was induced). COX-2 expression in the contralateral cortices and in control samples (group C) was faint. **(B)** Expression ratios of COX-2 in each group. The expression ratio of the cortex ipsilateral to the cortex in which SD was induced was significantly higher than that measured in group C ($P = 0.02$). **(C)** Immunoblot analysis revealed a 70- to 72-kd COX-2–immunoreactive band that is clearly seen in the SD group but that is barely detectable in group C. **(D)** Mirror section images immunostained for COX-2 (i) and microtubule-associated protein 2 (MAP-2; ii) are shown. Immunoreactive COX-2 and MAP-2 were localized in the same neurons; cell bodies and apical dendrites showed immunoreactivity. Scale bars: 200 μm.

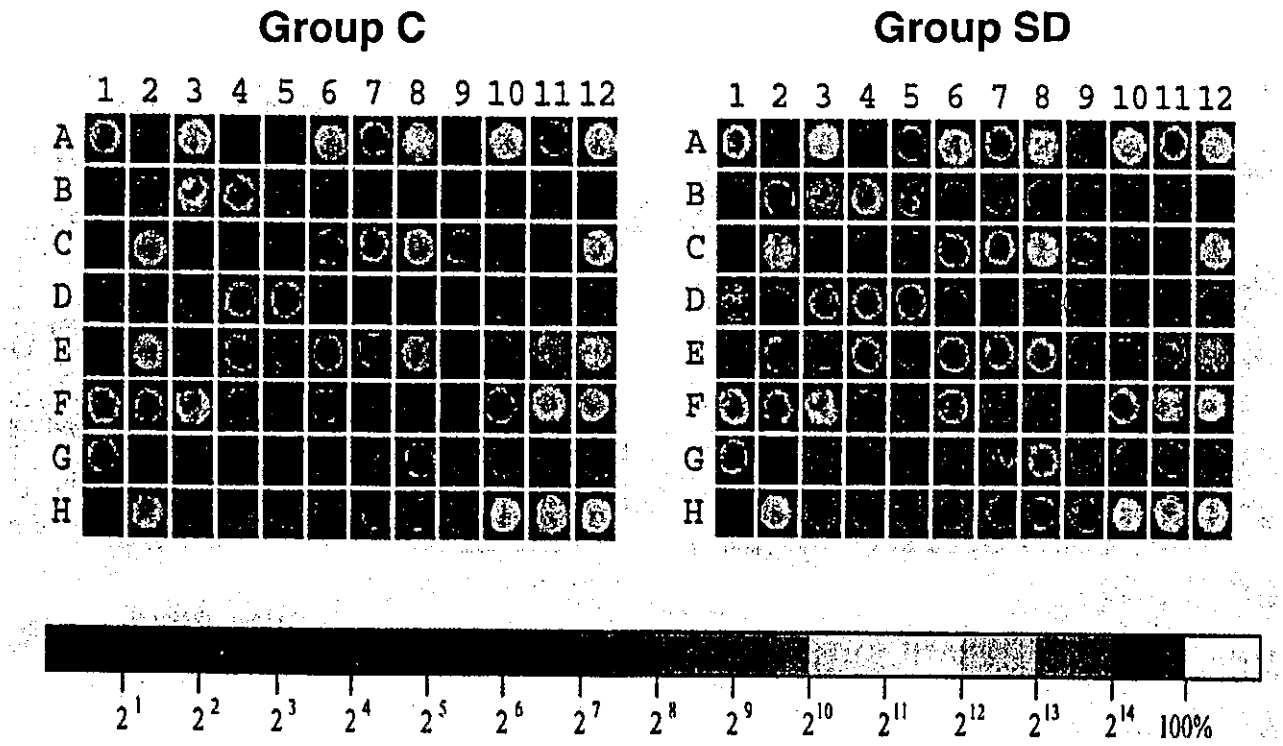

Nogawa et al., 1997) and that prevention of COX-2 expression might be beneficial in treating human ischemic stroke. Ischemia-related SDs have been regarded as good targets for pharmacologic intervention in stroke because they exacerbate the preexisting energy depletion in the periinfarct zone (Hossmann, 1994; Takano et al., 1996). Cyclooxygenase-2 was induced after SD and as a result of focal brain ischemia in rat models (Koistinaho et al., 1999; Miettinen et al., 1997). Koistinaho and Chan (2000) reported that SD directly induced COX-2 expression in focal brain ischemia by stimulating the NMDA receptor and activating phospholipase A_2. Only a few postmortem studies, however, reported COX-2 expression in human brain ischemia (Iadecola et al., 1999; Sairanen et al., 1998).

In our study, COX-2 was induced in the cortices that experienced SD, supporting previous observations in rodents (Koistinaho et al., 1999; Miettinen et al., 1997). Cyclooxygenase-2 gene expression increased by 1.6-fold in the SD group, as detected using a DNA microarray. The gene transcribing basic transcription element–binding protein 1, a thyroid hormone–regulated gene found in the developing rat brain, was also upregulated (Cayrou et al., 2002); the relation between this protein and SD remains to be clarified. Enard et al. (2002) showed numerous quantitative differences in gene expression between closely related mammalian species. Because they showed that such differences were particularly pronounced in the human brain, primate cDNA arrays analysis will need to be improved before we can fully identify candidate genes that may be involved in SD. In summary, as in rodents, neuronal COX-2 is induced in the primate cortex in response to SD.

Acknowledgments: The authors thank Dr. Toshiho Ohtsuki for his scientific input.

REFERENCES

Cayrou C, Denver RJ, Puymirat J (2002) Suppression of the basic transcription element–binding protein in brain neuronal cultures inhibits thyroid hormone-induced neurite branching. *Endocrinology* 143:2242–2249

Collaco-Moraes Y, Aspey B, Harrison M, Belleroche JD (1996) Cyclooxygenase-2 messenger RNA induction in focal cerebral ischemia. *J Cereb Blood Flow Metab* 16:1366–1372

Enard W, Khaitovich P, Klose J, Zollner S, Heissig F, Giavalisco P, Niselt-Struwe K, Muchmore E, Varki A, Ravid R, Doxiadis GM, Bontrop RE, Paabo S (2002) Intra- and interspecific variation in primate gene expression patterns. *Science* 296:340–343

Gidlund M, Orn A, Pattengale PK, Jansson M, Wigzell H, Nilsson K (1981) Natural killer cells kill tumor cells at a given stage of differentiation. *Nature* 292:848–850

Gill R, Andine P, Hillered L, Persson L, Hagberg H (1992) The effect of MK-801 on cortical spreading depression in the penumbral zone following focal ischemia in the rat. *J Cereb Blood Flow Metab* 12:371–379

Hossmann KA (1994) Viability thresholds and the penumbra of focal ischemia. *Ann Neurol* 36:557–565

Iadecola C, Forster C, Nogawa S, Clark HB, Ross ME (1999) Cyclooxygenase-2 immunoreactivity in the human brain following cerebral ischemia. *Acta Neuropathol* 98:9–14

Iijima T, Mies G, Hossmann KA (1992) Repeated negative DC deflections in rat cortex following middle cerebral artery occlusion are abolished by MK-801: effect on volume of ischemic injury. *J Cereb Blood Flow Metab* 12:727–733

Inoue H, Yokoyama C, Hara S, Tone Y, Tanabe T (1995) Transcriptional regulation of human prostaglandin-endoperoxide synthase-2 gene by lipopolysaccharide and phorbol ester in vascular endothelial cells. *J Biol Chem* 270:24965–24971

Koistinaho J, Chan PH (2000) Spreading depression-induced cyclooxygenae-2 expression in the cortex. *Neurochem Res* 25:645–651

Koistinaho J, Pasonen S, Yrjanheikki J, Chan PH (1999) Spreading depression-induced gene expression is regulated by plasma glucose. *Stroke* 30:114–119

Kuge Y, Hasegawa Y, Yokota C, Minematsu K, Hashimoto N, Miyake Y, Yamaguchi T (2000) Effects of single and repetitive spreading depression on cerebral blood flow and glucose metabolism in cats: a PET study. *J Neurol Sci* 176:114–123

Lauritzen M, Jorgensen MB, Diemer NH, Gjedde A, Hansen AJ (1982) Persistent oligemia of rat cerebral cortex in the wake of spreading depression. *Ann Neurol* 12:469–474

Lauritzen M, Olsen TS, Lassen NA, Paulson OB (1983) Changes in regional cerebral blood flow during the course of classic migraine attacks. *Ann Neurol* 13:633–641

Lyer VR, Eisen MB, Ross DT, Schuler G, Moore T, Lee JCF, Trent JM, Staudt LM, Hudson J, Boguski MS, Lashkari D, Shalon D, Botstein D, Brown PO (1999) The transcriptional program in the response of human fibroblasts to serum. *Science* 283:83–87

Miettinen S, Fusco FR, Yrjanheikki J, Keinanen R, Hirvonen T, Roivainen R, Narhi M, Hokfelt T, Koistinaho J (1997) Spreading depression and focal brain ischemia induce cyclooxygenase-2 in cortical neurons through *N*-methyl-D-aspartic acid-receptors and phospholipase A_2. *Proc Natl Acad Sci U S A* 94:6500–6505

Niwa K, Araki E, Morham SG, Ross ME, Iadecola C (2000) Cyclooxygenase-2 contributes to functional hyperemia in whisker-barrel cortex. *J Neurosci* 20:763–770

Nogawa S, Zhang F, Ross ME, Iadecola C (1997) Cyclo-oxygenase-2 gene expression in neurons contributes to ischemic brain damage. *J Neurosci* 17:2746–2755

Olesen J, Larsen B, Lauritzen M (1981) Focal hyperemia followed by spreading oligemia and impaired activation of rCBF in classic migraine. *Ann Neurol* 9:344–352

Piper RD, Lambert GA, Duckworth JW (1991) Cortical blood flow changes during spreading depression in cats. *Am J Physiol* 261:H96–H102

Sairanen T, Ristimaki A, Karjalainen-Lindsberg M-L, Paetau A, Kaste M, Lindsberg PJ (1998) Cyclooxygenase-2 induced globally in infarcted human brain. *Ann Neurol* 43:738–747

Takano K, Latour LL, Formato JE, Carano RAD, Helmer KG, Hasegawa Y, Sotak CH, Fisher M (1996) The role of spreading depression in focal ischemia evaluated by diffusion mapping. *Ann Neurol* 39:308–318

Woods RP, Iacoboni M, Mazziotta JC (1994) Bilateral spreading cerebral hypoperfusion during spontaneous migraine headache. *New Engl J Med* 331:1689–1692

Yokota C, Kuge Y, Hasegawa Y, Tagaya M, Abumiya T, Ejima N, Tamaki N, Yamaguchi T, Minematsu K (2002) Unique profile of spreading depression in a primate model. *J Cereb Blood Flow Metab* 22:835–842

ELSEVIER

Neuroscience Letters 357 (2004) 219–222

Neuroscience Letters

www.elsevier.com/locate/neulet

Temporal and topographic profiles of cyclooxygenase-2 expression during 24 h of focal brain ischemia in rats

Chiaki Yokota[a,*], Tomohito Kaji[b], Yuji Kuge[c], Hiroyasu Inoue[d], Nagara Tamaki[b], Kazuo Minematsu[e]

[a]*Cerebrovascular Laboratory, Department of Pathogenesis, National Cardiovascular Center Research Institute, 5-7-1 Fujishirodai, Suita, Osaka, 565-8565, Japan*

[b]*Department of Nuclear Medicine, Graduate School of Medicine, Hokkaido University, Sapporo, Japan*

[c]*Department of Patho-functional Bioanalysis, Graduate School of Pharmaceutical Sciences, Kyoto University, Kyoto, Japan*

[d]*Division of Molecular Pharmacology, Department of Pharmacology, National Cardiovascular Center Research Institute, Osaka, Japan*

[e]*Cerebrovascular Division, Department of Medicine, National Cardiovascular Center, Osaka, Japan*

Received 6 October 2003; received in revised form 17 December 2003; accepted 26 December 2003

Abstract

Substantial increases in cyclooxygenase-2 (COX-2) mRNA and protein levels were demonstrated in the peri-infarct and focal ischemic areas after 3–24 and 12–24 h, respectively, in rats. In the ischemic core, significant increases in COX-2 mRNA followed 6 h of ischemia, though the peak level was about one-third of that in the peri-infarct area. Increases in COX-2 protein in the ischemic core were not observed during ischemic periods. Diffuse, neuronal COX-2 staining was found in peri-infarct areas as well as in discrete, immunoreactive neurons in the ischemic core. Robust increases in prostaglandin E_2 levels in the peri-infarct area were demonstrated following 24 h of ischemia. Prostaglandin production as well as COX-2 expression in ischemic tissues depended on the degree and duration of the reduction in cerebral blood flow.

Keywords: Cyclooxygenase-2; Focal brain ischemia; Prostaglandin E_2; 6-keto-PG $F_{1\alpha}$; Cerebral blood flow; Rat

Cyclooxygenase-2 (COX-2), a rate-limiting enzyme in prostaglandin synthesis, is rapidly induced by proinflammatory cytokines in vitro and has been shown to mediate the induction of prostaglandin synthesis during the inflammatory response in vivo [17]. Accumulating evidence suggests that inflammatory processes play a role in the development and progression of atherosclerosis [2,8,14] and COX-2 in particular has become the focus of attention as a therapeutic target enzyme in acute coronary syndromes [1] and Alzheimer's disease [16]. We previously reported that neuronal COX-2 was induced within potentially viable hypoperfused brain areas after a 24 h ischemic period in non-human primates [20]. The role of neuronal COX-2 within such peri-infarct areas, however, is still unclear. Several reports using various rodent models suggested that COX-2 played a role in the development of ischemic injury [3,4,12]. A few postmortem reports suggested that the production of prostanoids by COX-2 after acute ischemia could contribute to the remodeling of neural networks that is seen after focal infarction [15]. The objective of the present study was to elucidate the topography and time course of COX-2 expression and prostaglandin (PG) E_2 (the major prostanoid involved in inflammation) production, as well as the production of the prostacyclin metabolite 6-keto-PG $F_{1\alpha}$ [11,13] during 24 h of focal brain ischemia.

Male Sprague–Dawley rats (300–350 g, $n = 40$) were used in this study. All procedures were approved by our Institutional Animal Research Committee and were performed in accordance with the standards published by the National Research Council. Rats were anesthetized with chloral hydrate (400 mg/kg body weight i.p.) and focal brain ischemia was produced by the intraluminal occlusion of the ostium of the right middle cerebral artery with nylon monofilaments, as previously described [7,9]. Rectal temperatures were monitored and maintained at around 37

* Corresponding author. Tel.: +81-6-6833-5012; fax: +81-6-6872-8091.
E-mail address: cyokota@ri.ncvc.go.jp (C. Yokota).

0304-3940/03/$ - see front matter © 2003 Elsevier Ireland Ltd. All rights reserved.
doi:10.1016/j.neulet.2003.12.109

°C with the aid of heating pads. Rats were sacrificed under chloral hydrate anesthesia at time 0 and at different times points after arterial occlusion (1, 2, 3, 4, 6, 8, 12, and 24 h, $n = 4$-5/time point) and their brains immediately immersed in ice-cold saline. The brains were then cut into four coronal sections (blocks A–D) as shown in Fig. 1A. Several blocks were frozen in isopentane-dry ice and stored at −80 °C until use, whereas others (from C) were embedded in paraffin for immunohistochemistry. Analysis of COX-2 expression (mRNA, protein), and measurement of the concentrations of PGE_2 and the prostacyclin metabolite 6-keto-PG $F_{1\alpha}$ in the peri-infarct areas and the ischemic core were performed using blocks A and C, respectively.

In some animals, *N*-isoproryl-*p*-[^{125}I]-iodoamphetamine ([^{125}I]IMP) (2.22 MBq/kg body weight) was injected into the femoral vein 5 min before sacrifice and ex vivo autoradiography was performed to measure cerebral blood flow (CBF) using blocks B and D. For each frozen block, tissues that were adjacent to block C were serially sectioned (20 μm). Exposure was carried out for 7 days in order to visualize the distribution of [^{125}I]IMP. The autoradiograms were analyzed using a computerized imaging analysis system (Bio-imaging Analyzer BAS-5000, Fuji Photo Film, Tokyo, Japan). A total of four regions of interest (ROIs), as shown in Fig. 1B, were bilaterally and symmetrically positioned in the cerebral cortices in each coronal slice of blocks B and D. Asymmetry indices (AIs) were defined as the ratios of values for ROIs in the hemisphere ipsilateral to the arterial occlusion (right) to those of the contralateral homologous ROIs. AIs of the ischemic core were defined as a/d, whereas the AIs of the peri-infarct area were defined as b/c (Fig. 1B). An average AI value from blocks B and D was calculated for the CBF in each area of the ischemic core and peri-infarction areas.

RNA preparation and blot analysis were performed using cortices from blocks A (peri-infarct area) and C (ischemic core) as previously described [6]. For the immunoblot analyses, right cortical samples from block A (peri-infarct area) were obtained from each animal at time 0, and 3, 6, 12, and 24 h after ischemia ($n = 4$-5 for each period). The sample volumes, which were about 20 mg for each animal, were pooled together for each ischemic period. Right

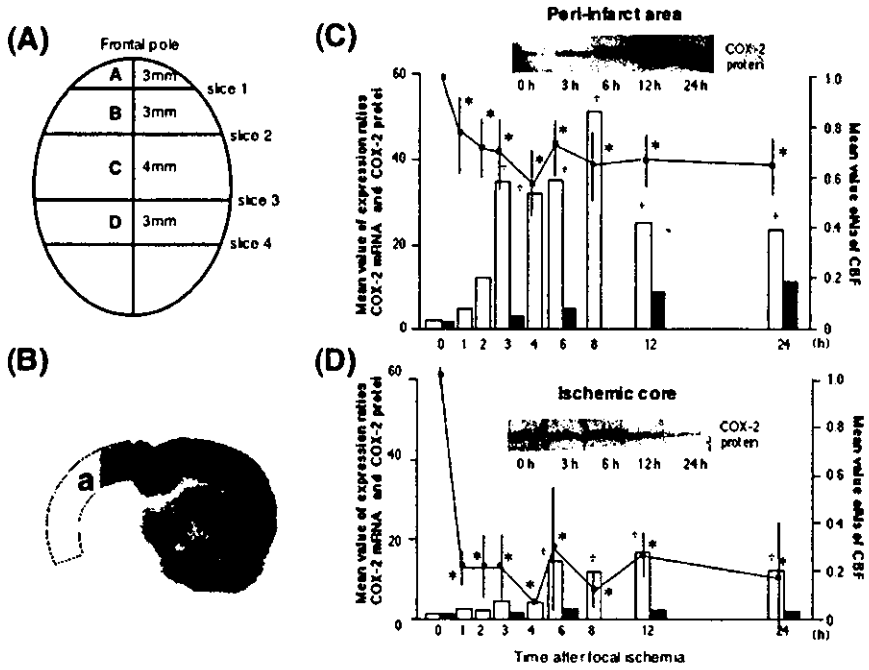

Fig. 1. Temporal profile of COX-2 expression associated with changes in CBF during 24 h of ischemia. (A) The brain was stereotaxically divided, on ice, into four coronal sections using a brain matrix. The first slice was made 3 mm from the frontal pole (block A), while the other three were cut at 3 mm (block B), 7 mm (block C), and 10 mm (block D) intervals posterior to the first slice. Determination of COX-2 expression levels (mRNA, protein) in the peri-infarct area and ischemic core was performed using blocks A and C, respectively. (B) To measure CBF in each animal, four regions of interest (ROIs) were bilaterally symmetrically placed on the cerebral cortices using coronal frozen slices from blocks B and D. Asymmetry indices (AIs) of the ischemic core were defined as a/d, whereas the AIs of the peri-infarct area were defined as b/c. (C,D) Lines indicate the mean AI values of CBF. The open and solid columns correspond to the mean expression ratios of COX-2 mRNA and COX-2 protein, respectively. Figures C and D show the time course of COX-2 expression in the peri-infarct area and ischemic core, respectively. A one-way ANOVA and post-hoc Fisher's tests were used to assess the differences in AIs and expression ratios of COX-2 mRNA between the different ischemic time points. CBF values in the peri-infarct area and ischemic core were significantly reduced compared to controls immediately after arterial occlusion ($^*P < 0.05$). The mean CBF values in the ischemic core and peri-infarct area were 0.19 ± 0.07 (mean ± SD) and 0.67 ± 0.06, respectively. The time course of COX-2 expression in the peri-infarct area was different from that in the ischemic core. Thus, the expression ratios of COX-2 mRNA increased significantly after 3 h of ischemia ($^\dagger P < 0.05$), with COX-2 protein also increasing with time in the peri-infarct area. On the other hand, significant increases in COX-2 mRNA were found 6 h after ischemia ($^\dagger P < 0.05$), and increases in COX-2 protein were not observed during the ischemic period in the ischemic core.

cortical samples from block C (ischemic core) for each ischemic period were also pooled together in this manner. Immunoblot analyses were then performed on each pooled sample as previously described [19]. COX-2 expression (mRNA, protein) in the ischemic cortices was calculated as expression ratios, defined as the ratio of the COX-2 mRNA or protein signals in the ischemic samples to their mean values in the corresponding control areas.

For immunohistochemistry, a mirror sectioning technique was used to colocalize COX-2 and microtubule-associated protein 2 (MAP-2), a neuronal skeletal protein, in sections from block C as previously described [19]. Negative controls consisted of sections that were incubated overnight without the primary antibody and processed as above.

Tissue concentrations of PGE_2 and 6-keto-PG $F_{1\alpha}$ in the right (ischemic) cortices of blocks A (peri-infarct area) and C (ischemic core) were determined using radioimmunoassay kits (Perkin-Elmer Life Sciences, Inc. MA, USA), and values were normalized for protein content.

Significant reductions in AIs for CBF in the peri-infarct area and ischemic core were demonstrated in animals at each ischemic time point compared to controls (Fig. 1C,D). The expression ratios of COX-2 mRNA increased significantly between 3 and 24 h of ischemia in the peri-infarct area compared to controls (Fig. 1C). In the ischemic core, significant increases in COX-2 mRNA were seen following 6 h of ischemia, which remained through 24 h (Fig. 1D). The peak value of the expression ratio of COX-2 protein in the peri-infarct area was 10.7 at 24 h of ischemia, while the peak expression ratio in the ischemic core was 2.0 at 6 h of ischemia.

COX-2 immunoreactive neurons were found predominantly in the peri-infarct area, though elevations in the immunohistochemical staining of discrete neuronal populations were also observed in the ischemic core (Fig. 2). Both COX-2 and MAP-2 immunoreactivity were abolished when the primary antibody was omitted.

Although no significant increases in PGE_2 and prostacyclin levels were observed in the peri-infarct and ischemic core areas following 3 h of ischemia, significant increases in prostaglandin levels were found in the ischemic hemisphere

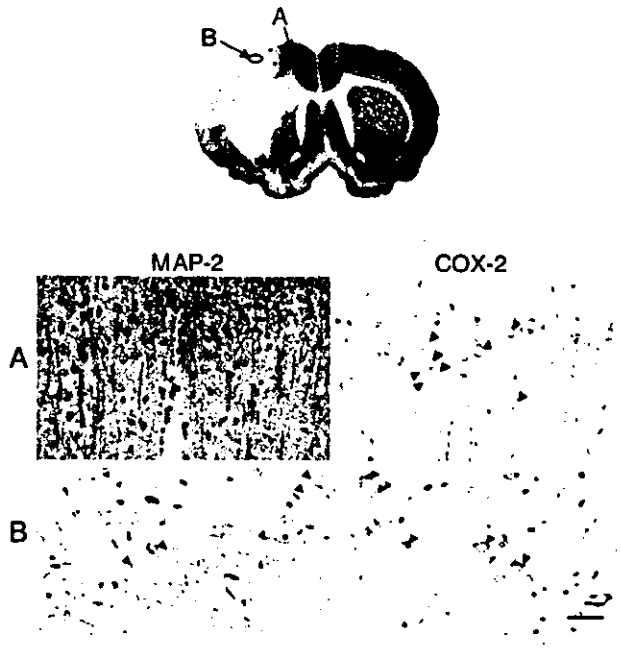

Fig. 2. Immunohistochemical analysis of COX-2. The single top figure shows a coronal slice of the brain of an animal that had undergone 3 h of ischemia, which was immunostained for microtubule-associated protein 2 (MAP-2). The bottom figures are sections that were immunostained for COX-2 and MAP-2 that were derived from either the peri-infarct area (region A in the top figure) or the ischemic core (B). Immunoreactive COX-2 and MAP-2 were localized in the same neurons in the ischemic core and peri-infarct area (arrow heads). Scale bar: 100 μm.

following 24 h of ischemia. In particular, PGE_2 levels in the peri-infarct area increased significantly (Table 1).

We previously demonstrated, in a small number of non-human primates, that post-ischemic COX-2 expression was regulated by the extent of CBF reduction [20]. In the present study, serial changes in the expression of COX-2 during focal ischemia were evaluated more closely in relation to the degree and duration of CBF reduction, and COX-2 reaction products (PGE_2 and prostacyclin), which were not analyzed in our previous study, were also examined. The time course of COX-2 expression in the ischemic core, characterized by a CBF of $<20\%$ of baseline values, was different from that seen in the peri-infarct area, where 70–80% of control CBF was observed following 24 h of ischemia. The upregulation

Table 1
Prostaglandin production (pg/mg total protein) in the right (ischemic) hemisphere

Prostaglandin	Duration of ischemia (h)	Peri-infarct area	Ischemic core
PGE_2	0	60.8 ± 16.6	21.4 ± 11.4
	3	156.6 ± 70.1	54.4 ± 22.3
	24	2609.0 ± 2522.0*†	414.6 ± 226.3*†
Prostacyclin metabolite (6-keto-PG $F_{1\alpha}$)	0	122.3 ± 47.6	47.6 ± 23.0
	3	200.8 ± 59.7	93.4 ± 43.5
	24	1143.0 ± 623.7*†	341.6 ± 84.5*†

*$P < 0.05$ vs. 0 h (control); †$P < 0.05$ vs. 3 h ischemia by ANOVA. The values are the mean ± SD.

of COX-2 mRNA in the peri-infarct area persisted for at least 24 h after ischemia, as did the production of COX-2 protein, which led to significant increases in prostacyclin as well as PGE_2 levels following 24 h of ischemia. In the ischemic core, increases in COX-2 mRNA persisted during the 24 h of ischemia, though significant increases in COX-2 protein were not observed. This latter finding was considered to be due to the severe ischemic injury that was caused by reduced CBF, which likely affected protein synthesis [5]. This assertion is supported by the work of Xie et al. [18] who reported that a CBF of $<70\%$ of controls suppressed protein synthesis. In spite of these effects on COX-2 protein, significant increases were seen in the concentration of prostaglandins in the ischemic core 24 h after ischemia. Local increases in neuronal COX-2 expression in the ischemic core, as determined by immunohistochemical analysis, could have accounted for this increase in prostaglandin concentration. Increases in PGE_2 in ischemic cortices after 24 h of ischemia, particularly in peri-infarct areas, were probably due to the upregulation of membrane-associated PGE_2 synthase (mPGES) activity as well as the induction of COX-2, which were reported to be essential components for delayed PGE_2 biosynthesis [10].

The induction of neuronal COX-2 is important for the regulation of prostaglandin signaling in post-ischemic regions, and the magnitude of COX-2 activity and prostaglandin production is determined by the degree and duration of CBF reduction. Before novel therapeutic options for stroke patients can be developed, further clarification of the effects of COX-2 during and after ischemia will be required.

Acknowledgements

This study was supported in part by a Grant-in-Aid for Scientific Research from the Japan Society for the Promotion of Science, by grants from the Takeda Medical Research Foundation, by the Mitsubishi Pharma Research Foundation, and by the Japan Heart Foundation.

References

[1] R. Altman, H.L. Luciardi, J. Muntaner, F.D. Rio, S.G. Berman, R. Lopez, C. Gonzalez, Efficacy assessment of meloxicam, a preferential cyclooxygenase-2 inhibitor, in acute coronary syndromes without ST-segment elevation: the Nonsteroidal Anti-Inflammatory Drugs in Unstable Angina Treatment-2 (NUT-2) pilot study, Circulation 106 (2002) 191–195.

[2] F.C. Barone, G.Z. Feuerstein, Inflammatory mediators and stroke: new opportunities for novel therapeutics, J. Cereb. Blood Flow Metab. 19 (1999) 819–834.

[3] Y. Collaco-Moraes, B. Aspey, M. Harrison, J. de-Belleroche, Cyclo-oxygenase-2 messenger RNA induction in focal cerebral ischemia, J. Cereb. Blood Flow Metab. 16 (1996) 1366–1372.

[4] K. Hara, D.L. Kong, F.R. Sharp, P.R. Weinstein, Effect of selective inhibition of cyclooxygenase 2 on temporary focal cerebral ischemia in rats, Neurosci. Lett. 256 (1998) 53–56.

[5] K.A. Hossmann, Viability thresholds and the penumbra of focal ischemia, Ann. Neurol. 36 (1994) 557–565.

[6] H. Inoue, C. Yokoyama, S. Hara, Y. Tone, T. Tanabe, Transcriptional regulation of human prostaglandin-endoperoxide synthase-2 gene by lipopolysaccharide and phorbol ester in vascular endothelial cells, J. Biol. Chem. 270 (1995) 24965–24971.

[7] Y. Kuge, K. Minematsu, T. Yamaguchi, Y. Miyake, Nylon monofilament for intraluminal middle cerebral artery occlusion in rats, Stroke 26 (1995) 1655–1658.

[8] P.L. McGeer, M. Schulzer, E.G. McGeer, Arthritis and anti-inflammatory agents as possible protective factors for Alzheimer's disease: a review of 17 epidemiologic studies, Neurology 47 (1996) 425–432.

[9] K. Minematsu, L. Li, M. Fisher, C.H. Sotak, M.A. Davis, M.S. Fiandaca, Diffusion weighted magnetic resonance imaging: rapid and quantitative detection of focal brain ischemia, Neurology 42 (1992) 235–240.

[10] M. Murakami, H. Naraba, T. Tanioka, N. Semmyo, Y. Nakatani, F. Kojima, T. Ikeda, M. Fueki, A. Ueno, S. Oh-ishi, I. Kudo, Regulation of prostaglandin E2 biosynthesis by inducible membrane-associated prostaglandin E2 synthase that acts in concert with cyclooxygenase-2, J. Biol. Chem. 275 (2000) 32783–32792.

[11] T. Murata, F. Ushikubi, T. Matsuoka, M. Hirata, A. Yamasaki, Y. Sugimoto, A. Ichikawa, Y. Aze, T. Tanaka, N. Yoshida, A. Ueno, S. Oh-ishi, S. Narumiya, Altered pain perception and inflammatory response in mice lacking prostacyclin receptor, Nature 388 (1997) 678–682.

[12] S. Nogawa, F. Zhang, M.E. Ross, C. Iadecola, Cyclo-oxygenase-2 gene expression in neurons contributes to ischemic brain damage, J. Neurosci. 17 (1997) 2746–2755.

[13] J.P. Portanova, Y. Zhang, G.D. Anderson, D.D. Hauser, J.L. Masferrer, K. Seibert, S.A. Gregory, P.C. Isakson, Selective neutralization of prostaglandin E2 blocks inflammation, hyperalgesia, and interleukin 6 production in vivo, J. Exp. Med. 184 (1996) 883–891.

[14] R. Ross, Atherosclerosis – an inflammatory disease, N. Engl. J. Med. 340 (1999) 115–126.

[15] T. Sairanen, A. Ristimaki, M.-L. Karjalainen-Lindsberg, A. Paetau, M. Kaste, P.J. Lindsberg, Cyclooxygenase-2 induced globally in infarcted human brain, Ann. Neurol. 43 (1998) 738–747.

[16] C. Scali, M.G. Giovannini, C. Prosperi, A. Bellucci, G. Pepeu, F. Casamenti, The selective cyclooxygenase-2 inhibitor rofecoxib suppresses brain inflammation and protects cholinergic neurons from excitotoxic degeneration in vivo, Neuroscience 117 (2003) 909–919.

[17] D.A. Willoughby, A.R. Moore, P.R. Colville-Nash, COX-1, COX-2, and COX-3 and the future treatment of chronic inflammatory disease, Lancet 355 (2000) 646–648.

[18] Y. Xie, G. Mies, K.A. Hossmann, Ischemic threshold of brain protein synthesis after unilateral carotid artery occlusion in gerbils, Stroke 20 (1989) 620–626.

[19] C. Yokota, H. Inoue, Y. Kuge, T. Abumiya, M. Tagaya, Y. Hasegawa, N. Ejima, N. Tamaki, K. Minematsu, Cyclooxygenase-2 expression associated with spreading depression in a primate model, J. Cereb. Blood Flow Metab. 23 (2003) 395–398.

[20] C. Yokota, Y. Kuge, H. Inoue, M. Tagaya, G. Kito, T. Susumu, N. Tamaki, K. Minematsu, Post-ischemic cyclooxygenase-2 expression is regulated by the extent of cerebral blood flow reduction in non-human primates, Neurosci. Lett. 341 (2003) 37–40.

Characterisation of [^{123}I]iomazenil distribution in a rat model of focal cerebral ischaemia in relation to histopathological findings

Tomohito Kaji[1], Yuji Kuge[2], Chiaki Yokota[3], Masafumi Tagaya[5], Hiroyasu Inoue[4], Tohru Shiga[1], Kazuo Minematsu[6], Nagara Tamaki[1]

[1] Department of Nuclear Medicine, Hokkaido University Graduate School of Medicine, Kita-ku, Sapporo, Japan
[2] Department of Tracer Kinetics, Hokkaido University Graduate School of Medicine, Kita-ku, Sapporo, Japan
[3] Department of Pathogenesis, Research Institute, National Cardiovascular Center, Suita, Osaka, Japan
[4] Department of Pharmacology, Research Institute, National Cardiovascular Center, Suita, Osaka, Japan
[5] Department of Internal Medicine, National Osaka Hospital, Chuo-ku, Osaka, Japan
[6] Cerebrovascular Division, Department of Medicine, National Cardiovascular Center, Suita, Osaka, Japan

Received: 14 May 2003 / Accepted: 27 July 2003 / Published online: 8 October 2003

Abstract. Iodine-123 labelled iomazenil ([^{123}I]IMZ) has been reported to be a useful marker of neuronal viability. The brain distribution of [^{123}I]IMZ, however, has not been correlated with the pathophysiological response in detail after an ischaemic insult. To characterise [^{123}I]IMZ as a marker of neuronal viability, we compared its brain distribution with cyclooxygenase-2 (COX-2) expression, DNA fragmentation and cellular integrity. [^{123}I]IMZ and [^{125}I]IMP were injected into rats with focal cerebral ischaemia for the purpose of dual-tracer autoradiography. COX-2 and microtubule-associated protein-2 (MAP-2, a marker of cellular integrity) were immunostained. In situ DNA polymerase-I-dependent dUTP incorporation into damaged DNA was used as an indicator of DNA fragmentation. Lesion to normal ratios (LNRs) for [^{123}I]IMP and [^{125}I]IMZ were calculated. [^{123}I]IMZ accumulation was preserved in several regions with impaired [^{123}I]IMP accumulation. COX-2 expression was occasionally observed, whereas neither DNA fragmentation nor MAP-2 denaturation was detected in these regions. DNA fragmentation and impaired MAP-2 immunostaining were observed only in the regions with reduced LNRs for both tracers. The LNR for [^{123}I]IMZ was significantly lower in regions with impaired MAP-2 immunostaining (0.120±0.152, P<0.0001), in regions positive for dUTP incorporation (0.488±0.166, P<0.0001) and in regions positive for COX-2 expression (0.626±0.186, P<0.001) than in histologically normal regions (0.784±0.213). Thus, neuronal DNA is still intact and cellular integrity is maintained in the ischaemic regions with preserved [^{123}I]IMZ accumulation. The impairment of [^{123}I]IMZ accumulation precedes DNA fragmentation and denaturation of cellular integrity. These results provide the molecular basis of [^{123}I]IMZ distribution.

Keywords: [^{123}I]iomazenil – Cerebral ischaemia – Neuronal viability – Cyclooxygenase-2 – DNA fragmentation

Eur J Nucl Med Mol Imaging (2004) 31:64–70
DOI 10.1007/s00259-003-1319-6

Nagara Tamaki (✉)
Department of Nuclear Medicine,
Hokkaido University Graduate School of Medicine,
Kita 15 Nishi 7, 060-8638 Kita-ku, Sapporo, Japan
e-mail: natamaki@med.hokudai.ac.jp
Tel.: +81-11-7065150, Fax: +81-11-7067155

Introduction

An ischaemic stroke is one of the most common neuronal disorders, and the number of patients suffering from the disease is increasing. For the clinical evaluation of ischaemic stroke, it is very important to precisely detect the ischaemic penumbra, which is an ischaemically affected but still viable tissue, because the penumbral tissue can be salvaged by pharmacological and/or surgical interventions [1, 2, 3, 4].

Iodine-123 iomazenil ([^{123}I]IMZ) is a probe for central-type benzodiazepine receptor (BZR) for single-photon emission tomography (SPET). Since GABA receptors are abundant in the cortex and sensitive to ischaemic damage, specific radioligands to their subunits, the cerebral BZRs existing in GABA-A receptors, can be used as a marker of neuronal viability [5]. Thus, BZR imaging with [^{123}I]IMZ should be useful for detecting viable neurons, which may help detect the penumbra after an isch-

aemic insult. In this regard, several experimental and clinical investigators have compared the [^{123}I]IMZ distribution with the cerebral blood flow, oxygen metabolism and/or glucose metabolism, and shown the potential of [^{123}I]IMZ for evaluation of neuronal viability after an ischaemic stroke [3, 6, 7, 8, 9, 10, 11, 12]. A few authors [6, 10, 11] have also correlated [^{123}I]IMZ distribution with histological findings obtained using the haematoxylin-eosin stain.

To the best of our knowledge, however, the brain distribution of [^{123}I]IMZ has not been correlated with the molecular response after an ischaemic insult in detail. The pathophysiological significance of findings that are actually imaged by [^{123}I]IMZ also remains to be elucidated. Accordingly, we compared the brain distribution of [^{123}I]IMZ with (1) cerebral blood flow, (2) the expression of cyclooxygenase-2 (COX-2), (3) fragmentation of DNA and (4) cellular integrity, in order to characterise [^{123}I]IMZ as a marker of neuronal viability. COX-2, a prostanoid synthesising enzyme, is expressed early after an ischaemic insult and contributes to the progression of ischaemic damage [13, 14, 15, 16, 17]. Thus, we examined COX-2 expression to evaluate the neuronal response early after an ischaemic insult. In situ DNA polymerase-I-dependent dUTP incorporation into damaged DNA was used as an indicator of DNA fragmentation. Techniques for visual detection and localisation of DNA injury/repair in situ include: TdT-dependent dUTP labelling of free 3'-OH ends of double-stranded DNA (TUNEL); Klenow fragment of DNA polymerase-I-dependent labelling of staggered 3'-OH ends and gaps; and DNA polymerase-I incorporation in nicks, gaps and staggered 3'-OH ends [18]. Of these, only DNA polymerase-I has 5'–>3' exonucleolytic activity, which allows nick translation and visualisation of randomly occurring single-strand scission of double-stranded DNA. MAP-2, a cellular structural protein existing on the surface of neurodendrites, is also immunostained as a marker of cellular integrity.

Materials and methods

Animal preparation. The experimental protocol was fully approved by the Laboratory Animal Care and Use Committee of Hokkaido University. Male Sprague-Dawley rats weighing 300–350 g were used. The rats had free access to water and laboratory chow. The animals were initially anaesthetised with 400 mg/kg body weight IP chloral hydrate. The body temperatures were monitored with rectal probes and maintained at 37°C with heating pads during the operation. The rats were subjected to permanent unilateral major artery occlusion. The right middle cerebral artery (MCA) of each rat was occluded intraluminally according to a method described in detail previously [19, 20, 21]. The rats were allowed to recover from anaesthesia and any induced neurological deficits were confirmed. The animals not showing any neurological deficits were excluded from this experiment.

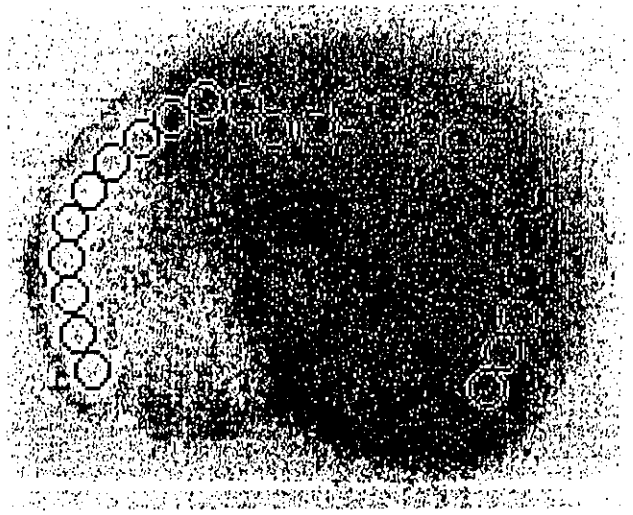

Fig. 1. An example of regions of interest (ROIs) on a coronal image. Twelve circular ROIs (2 mm in diameter) were determined on each hemisphere of the cortex symmetrically

Autoradiographic studies. The brain distributions of [^{123}I]IMZ and [^{125}I]IMP were determined using a dual-tracer autoradiographic technique. [^{123}I]IMZ (111 MBq/kg body weight) was first injected via the femoral vein 60 min before decapitation, to determine specific [^{123}I]IMZ distribution according to the methods reported by Toyama et al. [10, 11]. Then, 55 min later, [^{125}I]IMP (2.22 MBq/kg body weight) was injected via the contralateral femoral vein, to assess blood flow distribution [10, 11]. The rats were decapitated under chloral hydrate anaesthesia 5 min after the injection of [^{125}I]IMP, which was 2, 3, 4, 6, 8, 12 and 24 h after the ischaemic insult (n = four to six in each group). Their brains were removed quickly and carefully, and immersed in ice-cold saline. The brains were then sectioned at 6 mm caudal from the frontal pole using a brain matrix (RBM-4000C, ASI Instruments, Warren, MI) to obtain coronal sections. The brain samples were embedded in a medium (Tissue-Tek, Sakura Finetechnical Co., Ltd., Tokyo, Japan), frozen in isopentane-dry ice, and cut into 20-μm sections with a cryostat (Bright Instrument Co., Ltd., Cambridgeshire, England). The first autoradiographic exposure was performed for 3 h to detect the distribution of [^{123}I]IMZ. The second exposure was initiated 7 days later and carried out for 7 days to visualise the distribution of [^{125}I]IMP.

Histological studies. Immunoreactivity to COX-2 and microtubule-associated protein-2 (MAP-2) were detected in frozen sections (10 μm thick) adjacent to those used for the autoradiographic studies, using a standard immunostaining procedure [23]. Briefly, after fixation in a cold 1:1 acetone-to-methanol mixture, the sections were incubated with a polyclonal anti-COX-2 antibody (Cayman Chemical; dilution 1:2,000) or a purified mouse monoclonal anti-MAP-2 antibody (BD Pharmingen, San Diego; dilution 1:400). The bound antibody was visualised by staining with avidin/biotin conjugate immunoperoxidase (Vector Laboratories, Inc., CA, USA) and 3,3'-diaminobenzidine tetrahydrochloride (DAB; Vectastain Elite Kit, Vector Laboratories, CA).

DNA fragmentation was also detected on the adjacent sections by incorporation of digoxigenin-dUTP using DNA polymerase-I according to the method previously described [18, 23]. To confirm the nuclear localisation of the label, some sections were counterstained with haematoxylin.

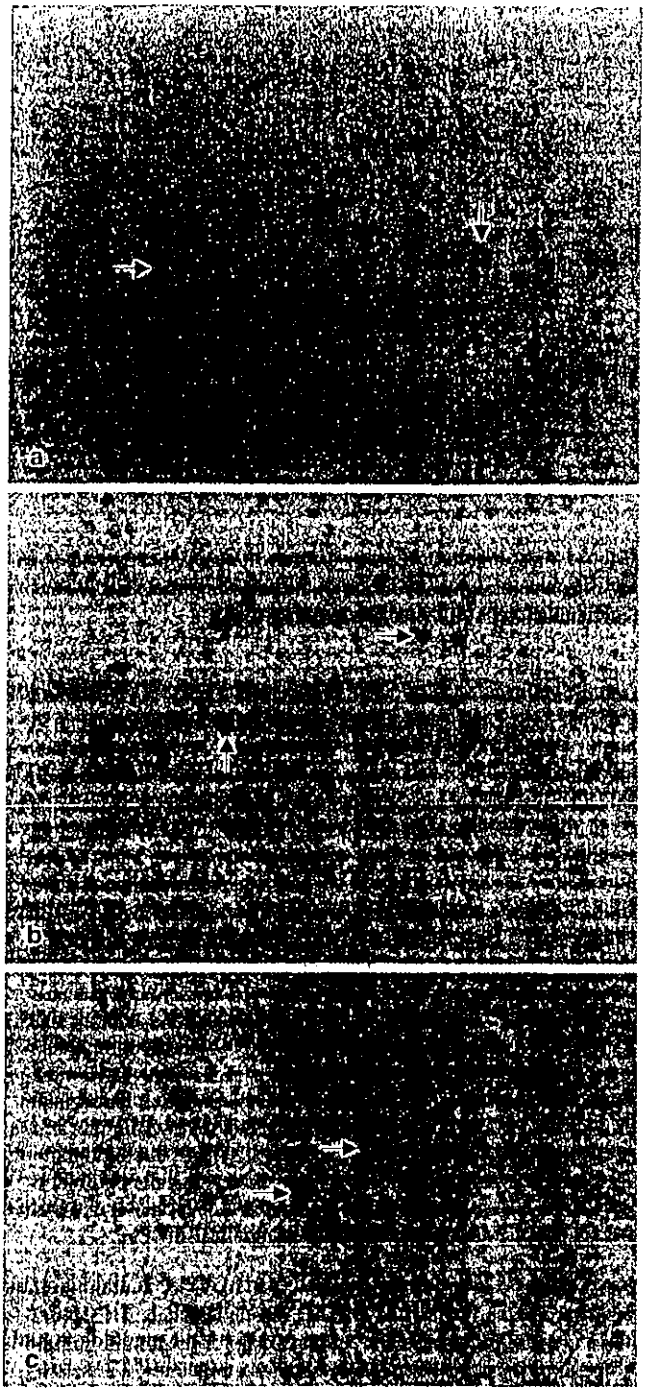

Data analysis. The autoradiograms were analysed using a computerised imaging analysis system (Bio-imaging Analyser BAS-5000, Fuji Photo Film, Tokyo, Japan). To quantitatively evaluate the distributions of [^{123}I]IMZ and [^{125}I]IMP, 12 circular regions of interest (ROIs, 2 mm in diameter) were determined on each hemisphere of the cerebral cortex in the autoradiograms symmetrically from the longitudinal fissure to the temporal lobe (Fig. 1). Lesion to normal ratios (LNRs) were defined as the ratios of values for an ROI in the lesioned hemisphere to those for the contralateral homologous ROI.

Based on the LNRs for [^{123}I]IMZ and [^{125}I]IMP, ROIs determined on the lesioned hemisphere were classified into three groups as shown in Table 1: group 1, LNRs for both [^{125}I]IMP and [^{123}I]IMZ were equal to or larger than 0.8; group 2, the LNRs for [^{125}I]IMP were less than 0.8 and those for [^{123}I]IMZ were equal to or larger than 0.8; group 3, LNRs for both [^{125}I]IMP and [^{123}I]IMZ were less than 0.8. A threshold LNR of 0.8 was chosen, considering the lesion detectability by the autoradiographic methods [11].

The ROIs determined on the lesioned hemisphere were also classified into four groups based on histological findings as follows (Fig. 2): group A, impaired MAP-2 immunostaining; group B, preserved MAP-2 immunostaining and positive for dUTP incorporation; group C, preserved MAP-2 immunostaining, negative for dUTP incorporation and positive for COX-2; group D, no histological evidence of an ischaemic injury.

All values are expressed as means or means ± standard deviation. A Z test was used to assess the significance of difference in the percentage of ROIs with impaired [^{125}I]IMP or [^{123}I]IMZ accumulation. One-way ANOVA and post-hoc tests (Fisher's method) were used to assess the significance of difference in the LNRs among the four groups classified on the basis of histological findings. A two-tail value of $P<0.05$ was considered to indicate statistical significance.

Results

Figure 3 shows representative autoradiograms for [^{125}I]IMP and [^{123}I]IMZ. The accumulation of [^{125}I]IMP decreased in a wide region in the MCA territory 2 h after occlusion, which extended with time. The region with

Fig. 2a–c. Representative images of **a** COX-2 immunostaining (×200), **b** dUTP incorporation (×200) and **c** MAP-2 immunostaining (×200). **a** Expression of COX-2 protein was occasionally observed (*arrows*). **b** The ring-like appearance (*arrows*) of dUTP incorporation shows the neuron on the way to apoptotic cell death. **c** Positive MAP-2 immunostaining (*arrows*) shows cellular integrity

Table 1. Histological findings in the three ROI groups classified on the basis of LNRs

Group	LNR_{IMP}	LNR_{IMZ}	Number (%) of ROIs		
			COX-2 (+)	dUTP (+)	MAP-2 (–)
Group 1 (n=14)	≥0.8	≥0.8	0 (0%)	0 (0%)	0 (0%)
Group 2 (n=24)	<0.8	≥0.8	4 (16.7%)	0 (0%)	0 (0%)
Group 3 (n=238)	<0.8	<0.8	79 (33.2%)	59 (24.8%)	176 (73.9%)

LNR_{IMP}, LNR for [^{125}I]IMP; LNR_{IMZ}, LNR for [^{123}I]IMZ; COX-2 (+), positive immunostaining for COX-2; dUTP (+), positive dUTP incorporation; MAP-2 (–), negative immunostaining for MAP-2

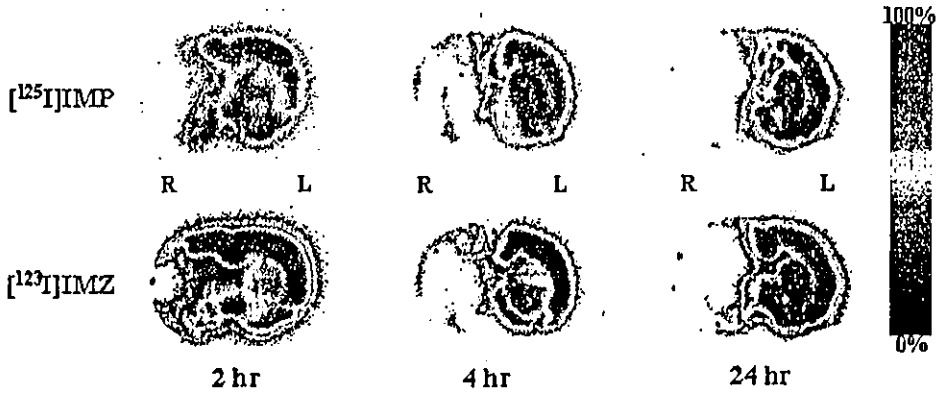

Fig. 3. Representative autoradiograms for [125I]IMP and [123I]IMZ

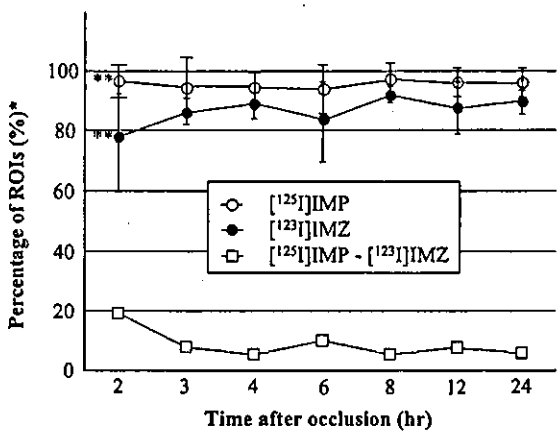

Fig. 4. Time course of the percentage of ROIs with impaired [125I]IMP or [123I]IMZ accumulation. *(Number of ROIs with LNRs less than 0.8)/(Number of total ROIs at each time point) ×100. ROIs with impaired [125I]IMP and [123I]IMZ accumulation were defined as those with LNRs less than 0.8. Significant uncoupling of accumulation between the two tracers was observed 2 h after occlusion (**P<0.01)

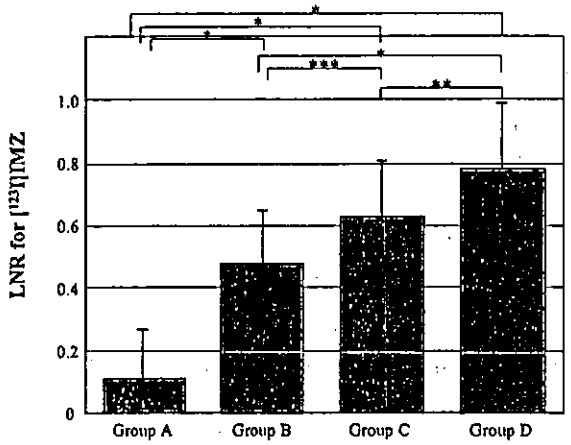

Fig. 5. The LNRs for [123I]IMZ in the four ROI groups classified on the basis of histological findings. Group A, impaired MAP-2 immunostaining; group B, preserved MAP-2 immunostaining and positive dUTP incorporation; group C, preserved MAP-2 immunostaining, negative dUTP incorporation and positive COX-2 immunostaining; group D, no histological evidence of ischaemic injury. Significant differences in LNRs between two groups: *P<0.0001, **P<0.001, ***P<0.01

decreased [123I]IMZ accumulation was smaller than that with decreased [125I]IMP accumulation (P<0.01). Uncoupling between [125I]IMP and [123I]IMZ accumulation was observed in regions surrounding the ischaemic core 2 h after occlusion, but such uncoupling reduced with time. The percentage of ROIs with impaired [123I]IMZ accumulation was significantly lower than that with decreased [125I]IMP accumulation at 2 h after occlusion (P<0.01), but not at other time points (Fig. 4).

Positivity for COX-2 was observed in 16.7% of the ROIs in the ischaemic lesions with preserved [123I]IMZ distribution (group 2) and 33.2% of the ROIs in the ischaemic lesions with decreased [123I]IMZ distribution (group 3), whereas no positivity for COX-2 was seen in non-ischaemic lesions (group 1) (Table 1). Neither positivity for dUTP incorporation nor decreased immunostaining of MAP-2 was observed in the ROIs in the lesions with preserved [123I]IMZ distribution (groups 1 and 2). Positivity for dUTP incorporation and impaired MAP-2 immunostaining were observed in 24.8% and 73.9% of the ROIs, respectively, in the lesions with decreased [123I]IMZ distribution (group 3) (Table 1).

When the ROIs were divided into four groups based on the histological findings (Fig. 5), the LNRs for [123I]IMZ in the lesions with preserved MAP-2 immunostaining (groups B, C and D) were significantly higher than those in the lesions with impaired MAP-2 immunostaining (group A; P<0.0001). The LNRs for [123I]IMZ in the lesions with preserved MAP-2 immunostaining and positive for dUTP incorporation (group B) were significantly lower than those in the lesions with preserved MAP-2 immunostaining and negative for dUTP incorporation (groups C; P<0.01, group D; P<0.0001). The LNRs for [123I]IMZ in the lesions with preserved MAP-2 immunostaining, negative for dUTP incorporation and positive for COX-2 (group C) were significantly lower

than those in the lesions with no histological evidence of an ischaemic injury (group D; $P<0.001$).

Discussion

In order to characterise [^{123}I]IMZ as a marker of neuronal viability, we compared the brain distribution of [^{123}I]IMZ with the expression of COX-2, DNA fragmentation and cellular integrity. Neither DNA fragmentation nor MAP-2 denaturation was detected in the ischaemic regions with preserved [^{123}I]IMZ accumulation. These results clearly demonstrate that neuronal DNA is still intact and cellular integrity is maintained in the ischaemic regions with preserved [^{123}I]IMZ accumulation. COX-2 expression was often observed in these regions. In addition, semiquantitative analysis based on the histological findings showed that [^{123}I]IMZ accumulation was significantly impaired in regions where DNA fragmentations were observed. Thus, [^{123}I]IMZ distribution can be an indicator that predicts the extent of neuronal damage after an ischaemic stroke.

In the present study, we compared the brain distribution of [^{123}I]IMZ with (1) CBF, (2) the expression of COX-2, a prostanoid synthesising enzyme that contributes to the progression of ischaemic damage [13, 14, 15, 16, 17], (3) fragmentation of DNA and (4) cellular integrity. The regions with preserved [^{123}I]IMZ accumulation and decreased [^{125}I]IMP accumulation, namely, uncoupling between CBF and BZR function, were observed 2 h after occlusion in regions surrounding the ischaemic core, which became smaller with time. Such uncoupling has been observed in the acute phase by several authors [9, 24, 25]. The BZR function in these regions can be regarded as intact in spite of hypoperfusion. Clinically, it was reported that the hypoperfused regions with preserved [^{123}I]IMZ accumulation do not develop infarction as determined in a follow-up evaluation with magnetic resonance imaging [3]. The uncoupling between [^{125}I]IMP and [^{123}I]IMZ accumulation may help determine the ischaemic penumbra.

Some authors [6, 10, 11] have compared [^{123}I]IMZ distribution with histological findings obtained using the haematoxylin-eosin stain. They suggested the potential of [^{123}I]IMZ for evaluating the extent of neuronal damage. The brain distribution of [^{123}I]IMZ, however, has not been correlated with the cellular response at the molecular level. The present results on the relationship between [^{123}I]IMZ accumulation and dUTP incorporation clearly demonstrate that neuronal DNA is still intact in the ischaemic regions where [^{123}I]IMZ accumulation is preserved. In addition, our results indicate the potential of [^{123}I]IMZ to significantly detect the region with DNA scission as a reduction in LNRs. It was reported that COX-2 is expressed early after an ischaemic insult and leads ischaemic neurons to apoptotic cell death [17, 26]. In the present study, COX-2 expression was often observed in the ischaemic regions with preserved [^{123}I]IMZ accumulation. COX-2 expression may precede impairment of [^{123}I]IMZ accumulation. On the other hand, the COX-2 protein was also observed in the regions where [^{123}I]IMZ accumulation decreased. The LNRs for [^{123}I]IMZ accumulation in group C (0.626±0.186) were significantly lower than those in group D (0.783±0.213). The role of the COX-2 protein may begin before the impairment of BZR function and it may continue even after this impairment, although further investigations are required to clarify this point. These results indicate that impairment of [^{123}I]IMZ accumulation may begin as early as the COX-2 expression after an acute stroke.

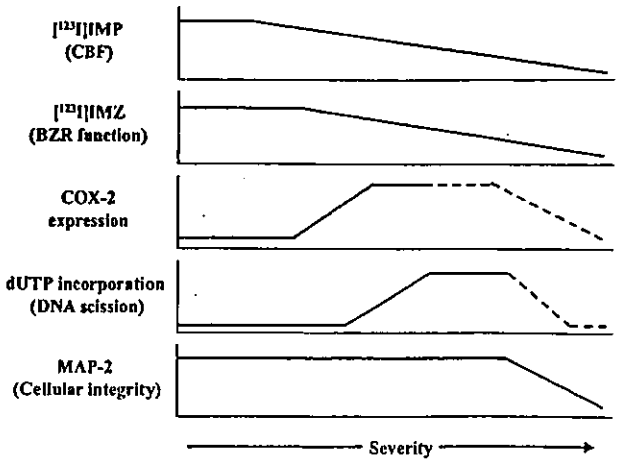

Fig. 6. Schematic representation of possible relationship between tracer accumulation and pathophysiological changes

From our results, a possible relationship between tracer accumulation and pathophysiological changes can be summarised as shown in Fig. 6. Namely, [^{125}I]IMP accumulation decreases concurrently with CBF after an ischaemic insult. COX-2 expression is often observed early after the ischaemic insult. [^{123}I]IMZ accumulation, namely, the BZR function, was impaired at a similar stage to COX-2 expression. DNA scission and impairment of cellular integrity follow the reduction in [^{123}I]IMZ accumulation.

Methodological considerations

In a clinical setting, an interval of several hours is required to sufficiently characterise BZR distribution after the [^{123}I]IMZ injection. In this study, however, rats were sacrificed 60 min after [^{123}I]IMZ administration, according to the method reported by Toyama et al. [10]. Their kinetic study indicated that specific binding of [^{123}I]IMZ can be evaluated 60 min after [^{123}I]IMZ injection in a rat model of cerebral ischaemia. Specific distribution of [^{123}I]IMZ can be achieved in a shorter period of 60 min in rats.

The relationship between tracer distribution and histological findings was evaluated simultaneously using all samples obtained from rats sacrificed at variable time intervals after the ischaemic insult, in order to characterise [^{123}I]IMZ distribution in regions with ischaemic injury of various extent. Regional analysis in rats subjected to the same period of MCA occlusion may provide more precise information on the relationship. The relatively narrow penumbra in rats, however, may restrict such evaluation and require a higher number of rats. Thus, in the present study, the relationship was evaluated simultaneously in rats sacrificed at variable time intervals.

The average LNR for [^{123}I]IMZ in histologically normal regions was not higher than 0.8. Although, in this study, we chose 0.8 as the threshold value of the LNRs for [^{123}I]IMZ, further examinations may be needed to determine a more suitable threshold value of LNR for [^{123}I]IMZ.

In the present study, we used a dual-tracer autoradiographic technique to evaluate the blood flow and [^{123}I]IMZ binding in the same individuals. Consequently, we could not perform quantitative assessment of the blood flow and [^{123}I]IMZ binding, as it is methodologically difficult to quantitatively assess flow and IMZ binding using the dual-tracer autoradiographic technique. Further studies, especially on quantitative measurement of flow and [^{123}I]IMZ binding, are required to confirm the present results and to obtain relevant information on the flow and [^{123}I]IMZ binding in relation to the histopathological findings.

Clinical implications

The routine use of nuclear medicine for the clinical assessment of neuronal viability has been limited exclusively to the determination of CBF, oxygen and/or glucose consumption, and CBF reactivity to acetazolamide. Oxygen and glucose metabolism and CBF reactivity to acetazolamide, however, do not provide direct information on neuronal viability. Rather, these techniques yield information not only on neurons but also on astrocytes and Schwann cells. On the other hand, [^{123}I]IMZ, a central-type BZR ligand, can be a specific marker of neuronal viability. Heiss et al. suggested that imaging of BZR receptors could distinguish between irreversibly damaged and viable penumbra tissues immediately after an acute stroke using carbon-11 flumazenil and positron emission tomography [27, 28]. The present study in the rat model demonstrated that [^{123}I]IMZ can also be a marker for neuronal viability. In addition, [^{123}I]IMZ does not require in-house cyclotrons and positron emission tomography, and can be commercially supplied. The availability of this procedure is expected to favour the clinical application of [^{123}I]IMZ.

Conclusion

The present study demonstrated for the first time that impairment of [^{123}I]IMZ accumulation precedes DNA fragmentation and denaturation of cellular integrity. Our results provide the molecular basis of [^{123}I]IMZ distribution. [^{123}I]IMZ accumulation can be a clue to predicting the severity of ischaemic neuronal injury.

Acknowledgement. The authors are grateful to Professors S. Nishi, K. Miyasaka and T. Ohnishi of the Central Institute of Isotope Science, Hokkaido University, for supporting this work. We also express gratitude to Drs. T. Abumiya and K. Hikosaka for helpful discussions.

This work was supported in part by a Grant-in-Aid for Scientific Research from the Japan Society for the Promotion of Science, and Grants from Japan Heart Foundation Research, the Takeda Medical Research Foundation in Japan and the Mitubishi Pharma Research Foundation in Japan.

References

1. Garcia JH, Lassen NA, Weiller C, Sperling B, Nakagawara J. Ischemic stroke and incomplete infarction. *Stroke* 1996; 27:761–765.
2. Garcia JH, Liu KF, Ye ZR, Gutierrez JA. Incomplete infarct and delayed neuronal death after transient middle cerebral artery occlusion in rats. *Stroke* 1997; 28:2303–2310.
3. Nakagawara J, Sperling B, Lassen NA. Incomplete brain infarction of reperfused cortex may be quantitated with iomazenil. *Stroke* 1997; 28:124–132.
4. Heiss WD, Graf R, Fujita T, Ohta K, Bauer B, Lötten J, Wienhard K. Early detection of irreversibly damaged ischemic tissue by flumazenil positron emission tomography in cats. *Stroke* 1997; 28:2045–2052.
5. Heiss WD, Kracht LW, Thiel A, Grond M, Pawlik G. Penumbral probability thresholds of cortical flumazenil binding and blood flow prediction tissue outcome in patients with cerebral ischaemia. *Brain* 2001; 124:20–29.
6. Odano I, Miyashita K, Minoshima S, Nakajima T, Fujita M, Takahashi N, Ikuta F. A potential use of a ^{123}I-labeled benzodiazepine antagonist as a predictor of neuronal call viability: comparisons with ^{14}C-labeled 2-deoxyglucose autoradiography and histological examination. *Nucl Med Commun* 1996; 16:443–446.
7. Matsuda H, Tsuji S, Kuji I, Shiba K, Hisada K, Mori H. Dual-tracer autoradiography using ^{125}I-iomazenil and ^{99m}Tc-HMPAO in experimental brain ischemia. *Nucl Med Commun* 1995; 16:581–590.
8. Hatazawa J, Shimosegawa E, Satoh T, Kanno I, Uemura K. Central benzodiazepine receptor distribution after subcortical hemorrhage evaluated by means of [^{123}I]IMZ and SPECT. *Stroke* 1995; 26:2267–2271.
9. Dong Y, Fukuyama H, Nabatame H, Yamauchi H, Shibasaki H, Yonekura Y. Assessment of benzodiazepine receptors using iodine-123-labeled iomazenil single-photon emission computed tomography in patients with ischemic cerebrovascular disease. A comparison with PET study. *Stroke* 1997; 28:1776–1782.
10. Toyama H, Matsumura K, Nakashima H, Takeda K, Takeuchi A, Koga S, Yoshida T, Ichise M. Characterization of neuronal

damage by iomazenil binding and cerebral blood flow in an ischemic rat model. *Ann Nucl Med* 1998; 12:267–273.
11. Watanabe Y, Nakano T, Yutani K, Nishimura H, Kusuoka H, Nakamura H, Nishimura T. Detection of viable cortical neurons using benzodiazepine receptor imaging after reversible focal ischaemia in rats: comparison with regional cerebral blood flow. *Eur J Nucl Med* 2000; 27:308–313.
12. al-Tikriti MS, Dey HM, Zoghbi SS, Baldwin RM, Zea-Ponce Y, Innis RB. Dual-isotope autoradiographic measurement of regional blood flow and benzodiazepine receptor availability following unilateral middle cerebral artery occlusion. *Eur J Nucl Med* 1994; 21:196–202.
13. Nogawa S, Zhang F, Ross ME, Iadecola C. Cyclo-oxygenase-2 gene expression in neurons contributes to ischemic brain damage. *J Neurosci* 1997; 17:2746–2755.
14. Sairanen T, Ristimaki A, Karjalainen-Lindsberg ML, Paetau A, Kaste M, Lindsberg PJ. Cyclooxygenase-2 is induced globally in infarcted human brain. *Ann Neurol* 1998; 43:738–747.
15. Iadecola C, Forster C, Nogawa S, Clark HB, Ross ME. Cyclooxygenase-2 immunoreactivity in the human brain following cerebral ischemia. *Acta Neuropathol (Berl)* 1999; 98:9–14.
16. Hewett SJ, Uliasz TF, Vidwans AS, Hewett JA. Cyclooxygenase-2 contributes to *N*-methyl-D-asparatate-mediated neuronal cell death in primary cortical cell culture. *J Pharmacol Exp Ther* 2000; 293:417–425.
17. Takedera T, Yumoto H, Tozuka Y, Ohyashiki T. Prostaglandin E(2) induces caspase-dependent apoptosis in rat cortical cells. *Neurosci Lett* 2002; 317:61–64.
18. Gavrieli Y, Sherman Y, Ben-Sasson SA. Identification of programmed cell death in situ via specific labeling of nuclear DNA fragmentation. *J Cell Biol* 1992; 119:493–501.
19. Longa EZ, Weinstein PR, Carlson S, Cummins R. Reversible middle cerebral artery occlusion without craniotomy in rats. *Stroke* 1989; 20:84–91.
20. Minematsu K, Li L, Fisher M, Sotak CH, Davis MA, Fiandaca MS. Diffusion-weighted magnetic resonance imaging:rapid and quantitative detection of focal brain ischemia. *Neurology* 1992; 42:235–240.
21. Kuge Y, Minematsu K, Yamaguchi T, Miyake Y. Nylon monofilament for intraluminal middle cerebral artery occlusion in rats. *Stroke* 1995; 26:1655–1658.
22. Sternberger LA, Sternberger NH. The unlabeled antibody method: comparison of peroxidase- antiperoxidase with avidin-biotin complex by a new method of quantification. *J Histochem Cytochem* 1986; 34:599–605.
23. Tagaya M, Liu K, Copeland B, Seiffert D, Engler R, Garcia JH, Zoppo GJ. DNA scission after focal brain ischemia/temporal differences in two species. *Stroke* 1997; 28:1245–1254.
24. Torizuka K, Uemura K, Toru M, Shinohara Y, Nishimura T, Yonekura Y, Nakagawara J, Matsuda H, Sakai F, Matsuda K, Fukuyama H, Morimoto K. A phase 3 clinical trial of ^{123}I-iomazenil, a new central-type benzodiazepine receptor imaging agent. Part 4. Report on clinical usefulness in diagnosis of cerebrovascular diseases. *Kaku Igaku* 1996; 33:329–344.
25. Moriwaki H, Matsumoto M, Hashikawa K, Oku N, Ishida M, Seike Y, Fukuchi K, Hori M, Nishimura T. Iodine-123-iomazenil and iodine-123-iodoamphetamine SPECT in major cerebral artery occlusive disease. *J Nucl Med* 1998; 39:1348–1353.
26. Matsuoka Y, Okazaki M, Zhao H, Asai S, Ishikawa K, Kitamura Y. Phosphorylation of c-Jun and its localization with heme oxygenase-1 and cyclooxygenase-2 in CA1 pyramidal neurons after transient forebrain ischemia. *J Cereb Blood Flow Metab* 1999; 19:1247–1255.
27. Heiss WD, Grond M, Thiel A, Ghaemi M, Sobesky J, Bauer B, Wienhard K. Permanent cortical damage detected by flumazenil positron emission tomography in acute stroke. *Stroke* 1998; 29:454–461.
28. Heiss WD, Kracht L, Grond M, Rudolf J, Bauer B, Wienhard K, Pawlik G. Early [^{11}C]flumazenil/H_2O positron emission tomography predicts irreversible ischemic cortical damage in stroke patients receiving acute thrombolytic therapy. *Stroke* 2000; 31:366–369.

ELSEVIER

Experimental Gerontology 38 (2003) 183–187

Experimental Gerontology

www.elsevier.com/locate/expgero

Brain ischemia as a potential target of gene therapy

Hiroaki Ooboshi*, Setsuro Ibayashi, Junichi Takada, Yasuhiro Kumai, Mitsuo Iida

Department of Medicine and Clinical Science, Graduate School of Medical Sciences, Kyushu University, 3-1-1 Maidashi, Higashi-ku, Fukuoka 812-8582, Japan

Received 29 April 2002; accepted 10 May 2002

Abstract

Brain infarction is one of the most important age-associated medical conditions, and the age-related neuronal vulnerability to brain ischemia is suggested to play an important role. Recent advancements in gene transfer techniques have provided promising approaches to the treatment of brain ischemia. In experimental studies, the ischemic penumbra area can be targeted by gene transfer even after ischemic insult, and post-ischemic gene therapy seems effective in attenuation of ischemic damage in both global and focal brain ischemia. Perivascular approaches of gene transfer to the cerebral blood vessels through the subarachnoid space may lead to prevention of brain ischemia caused by vasospasm after subarachnoid hemorrhage. Gene transfer to cerebral blood vessels and ischemic brain tissue may offer future therapeutic approaches to stroke.

Keywords: Gene therapy; Gene transfer; Brain; Ischemia; Aging; Stroke

1. Introduction

Gene transfer is an attractive method for studies of vascular and neuronal biology, and has been attempted for therapy of congenital and malignant diseases (Zabner et al., 1993; Abbott, 2001). Advancement of this technique, however, reveals clinical usefulness of gene therapy for cardiovascular disease (Isner, 2002). Furthermore, recent experimental data suggest that stroke, the most important cardiovascular medical condition in the elderly population, may be treated by gene therapy. In this article we focus on ischemic stroke as the age-associated disease and describe possibilities of gene therapy for brain ischemia.

2. Age-related ischemic vulnerability

Stroke is the third leading cause of death in the Western countries and Japan (Ueda et al., 1990), and aging is known as the main risk factors for stroke (Wolf et al., 1998) and vascular dementia (Ueda et al., 1992). Although aged models for the experimental brain ischemia have been claimed to be important (Millikan, 1992), the studies using such models are limited. We have developed experimental models for brain ischemia with aged spontaneously hypertensive rats, a very relevant model for human stroke, and demonstrated that the hippocampus in the aged rat was more susceptible to brain ischemia than that in the adult (Yao et al., 1991). Similar susceptibility of aged animals following embolic brain damage was also reported (Futrell et al., 1991).

Because reduction of cerebral blood flow (CBF) was similar between the adult and aged animals in the above model, factors other than blood flow were suggested to induce the ischemic damages in the aged animals. Massive increases of extracellular excitatory amino acids are an important determinant of ischemic damage (Benveniste et al., 1984) in the hippocampus and striatum, which are known to be vulnerable to ischemia (Kirino, 1982; Pulsinelli et al., 1982). In our model, however, no significant differences in ischemia-induced changes in excitatory amino acids between aged and adult animals could be observed (Yao et al., 1993). Interestingly, smaller increases of extracellular taurine, an inhibitory amino acid (Shurr et al., 1987), were found during ischemia in the hippocampus of the aged animals (Ooboshi et al., 1995a). Therefore, an imbalance between excitatory and inhibitory amino acids (Globus et al., 1991) may play a critical role in the age-related vulnerability of the hippocampus.

Brain hypothermia has been reported to exert marked neuroprotection against ischemic insults in the adult animals

* Corresponding author. Tel.: +81-92-642-5256; fax: +81-92-642-5271.
E-mail address: ooboshi@intmed2.med.kyushu-u.ac.jp (H. Ooboshi).

0531-5565/03/$ - see front matter © 2002 Elsevier Science Inc. All rights reserved.
PII: S0531-5565(02)00150-X

Table 1
Characteristics of gene transfer vectors

Vector	Plasmid alone	Retrovirus	Adenovirus	HSV	HVJ-liposome	AAV	Lentivirus
Efficiency	Low	Low	High	High	Moderate	Moderate	Moderate
Host range	Narrow	Narrow	Wide	Narrow	Wide	Wide	Wide
Expression period	Short	Long	Short	Short	Short	Long	Long
Mutagenesis	None	Possible	None	None	None	Possible	Possible
Toxicity	Low	Low	Some	Some	Low	Low	Low
Transferable DNA	Large	Small	Large	Large	Large	Small	Small

HSV, helpes simplex virus; HVJ, hemagglutinating virus of Japan; AAV, adeno-associated virus.

(Busto et al., 1987; Minamisawa et al., 1990). Because effects of hypothermia in the aged animals were not well defined, we examined the effects of mild brain hypothermia on the age-related brain damage to transient ischemia. Even small reduction of brain temperature (by 3 °C) markedly attenuated ischemic damages in the hippocampus (Ooboshi et al., 2001). Therefore, mild brain hypothermia may be a useful approach for treatment of brain infarction even in the elder population.

3. Gene transfer to ischemic brain

Several vectors for use in gene therapy have been proposed and each contains benefits and drawbacks (Table 1). Of these vectors, the most commonly used in the cardiovascular clinical trials is the recombinant adenovirus (Isner et al., 2001). The adenoviral vector consists of 36 kb DNA inside the capsid protein. Advantages of this vector are a wide host range, low probability of mutagenesis, and a high degree of successful gene transfer (Schneider et al., 1993; Trapnell, 1993).

Recently both brain infarction and ischemic heart disease have been cited as selected targets of gene therapy (Heistad and Faraci, 1996; Verma and Somia, 1997). However, most gene transfer approaches use host machinery for gene expression, and in ischemic conditions protein synthesis is impaired. Previous reports have revealed that protein synthesis starts to decline when CBF falls to less than 50% (Xie et al., 1989; Mies et al., 1993). Therefore, it is necessary to evaluate how brain ischemia would affect the efficiency of gene transfer. We examined effects of focal brain ischemia on transgene expression using the photothrombotic ischemic model which occludes the distal middle cerebral artery of spontaneously hypertensive rats with a platelet-rich thrombus. Our model produced a consistent size of brain infarction (Yao et al., 1996). When the adenoviral vector was directly injected into the ischemic and non-ischemic regions after induction of focal ischemia, transgene expression of the reporter gene was detected 1–7 days after ischemia, in both neurons and non-neuronal cells (Ooboshi et al., 2001). Although transgene expression in the ischemic core was poor, the peri-ischemic area, the presumable ischemic penumbra in our model, revealed good expression of the reporter gene. Analysis of blood flow at the penumbra area revealed that CBF threshold for transgene expression was approximately 40% of the resting value. Our results suggest that gene transfer to the ischemic penumbra area may be feasible for treatment of brain infarction.

Because direct gene transfer to the ischemic core seems difficult due to the limited efficacy, one alternative approach may be the transfer of genes that express releasable or diffusible products to the non-ischemic area (Ooboshi et al., 1997b; Ooboshi et al., 1998). This approach would overcome limitations of current techniques by allowing sufficient release of effective products in spite of marginally transfected cells. Administration of the adenoviral vectors in the lateral ventricle provides prominent gene expression at the ventricular wall (Ooboshi et al., 1995b), and gene transfer of interleukin-1 receptor antagonist to the ventricular wall was reported to reduce infarct size (Betz et al., 1995). Therefore, other anti-inflammatory cytokines and growth factors may be useful for the treatment of brain ischemia.

Table 2
Protection of brain ischemia by gene transfer

Gene	Vector	Ischemic model	Authors (year)
IL-1 receptor antagonist	Adenovirus	Focal ischemia	Betz et al. (1995)
bcl2	Herpes virus	Focal ischemia	Linnik et al. (1995)
Glucose transporter	Herpes virus	Focal ischemia	Lawrence et al. (1996)
NAIP	Adenovirus	Focal ischemia	Xu et al. (1997)
hsp72	Herpes virus	Focal ischemia	Yenari et al. (1998)
GDNF	Adenovirus	Focal ischemia	Kitagawa et al. (1999)
IL-1 receptor antagonist	Adenovirus	Global ischemia	Yang et al. (1999)
bcl2	AAV	Global ischemia	Shimazaki et al. (2000)
GDNF	Adenovirus	Global ischemia	Yagi et al. (2000)
SAG	Adenovirus	Focal ischemia	Yang et al. (2001)
HGF	HVJ-liposome	Global ischemia	Hayashi et al. (2001)
TGF-ss1	Adenovirus	Focal ischemia	Pang et al. (2001)
Calbindin D28K	Herpes virus	Focal ischemia	Yenari et al. (2001)

IL, interleukin; NAIP, neuronal apoptosis inhibitory protein; hsp, heat shock protein; GDNF, glial cell line-derived neurotrophic factor; SAG, sensitive to apoptosis gene; HGF, hepatocyte growth factor; TGF, transforming growth factor; AAV, adeno-associated virus; HVJ, hemagglutinating virus of Japan.

Several gene transfer approaches were reported to protect against brain ischemia in different models (Table 2), suggesting the use of gene therapy for brain ischemia. Recently we have observed that gene transfer to the aged ischemic brain is more efficient than when transfer occurs in adult ones (unpublished data). Thus, gene therapy to the aged ischemic brain, may be feasible, and these new therapeutic approaches may provide direction to develop procedures which may reduce or minimize disability in the aged population in the near future.

4. Gene transfer to cerebral blood vessels

Because stroke is caused by vascular lesions, cerebral blood vessels are important targets in acute and chronic treatment. In order to achieve gene transfer in cerebral blood vessels, intravascular administration of the vector with special catheters would be an ideal approach in a manner similar to techniques used in peripheral vessels (Nabel et al., 1990). However, needs for transient cessation of blood flow for the contact between vectors and vessels are obstacles for gene transfer to the cerebral circulation. One strategy to minimize this problem is shortening of the contact period by increasing the efficiency of gene transfer. Work is ongoing to modulate vector construct or addition of specific materials to enhance efficiency (Toyoda et al., 1998). Technological progress in this area would make it possible to use the intravascular approach for gene transfer to cerebral blood vessels (Ooboshi et al., 1997a).

Another alternative method for gene transfer to cerebral circulation is the perivascular approach (Rios et al., 1995). Vectors administered via the cisterna magna efficiently expressed transgene around the major cerebral arteries and adjacent tissue in several models (Ooboshi et al., 1997c; Christenson et al., 1998). Therefore, these perivascular approaches via the subarachnoid space may be feasible when the target of gene transfer is major cerebral vessels.

One of the most suitable applications of perivascular gene therapy is prevention of vasospasm after subarachnoid hemorrhage. Because vasospasm occurs several days after bleeding and the following brain ischemia is severe, gene therapy seems suitable for this disorder. The efficacy of gene transfer to the cerebral blood vessels after subarachnoid hemorrhage was acceptable even in the presence of subarachnoid clotting (Muhonen et al., 1997). Currently, transfer of the gene for vasodilatation, quenching of superoxide or inhibition of inflammatory process using the perivascular approach has been reported as effective in preventing vasospasm (Ono et al., 1998; Toyoda et al., 2000; Khurana et al., 2002; Watanabe et al., 2002). Therefore, perivascular approaches to the cerebral blood vessels may be useful in gene therapy for subarachnoid hemorrhage.

5. Conclusion

Brain infarction is one of the most important age-associated medical conditions. Recent developments in gene transfer techniques provide efficient transgene expression in the cerebral blood vessels and ischemic brains, including the aging brain. Although safety issues must be evaluated and additional research performed, it appears that brain ischemia is a potential target of gene therapy and advancement of gene transfer may provide a promising treatment for severe stroke.

Acknowledgements

This work was supported by the Grant-in-Aid from the Ministry of Health and Welfare Comprehensive Research on Aging and Health (H11-008), and from the Ministry of Education, Science and Culture (14570604), Tokyo, Japan. We would like to thank the University of Iowa Gene Transfer Vector Core, especially Beverly L. Davidson and Richard D. Anderson.

References

Abbott, A., 2001. Genetic medicine gets real. Nature 411, 410–412.

Benveniste, H., Drejer, J., Schousboe, A., Diemer, N.H., 1984. Elevation of the extracellular concentrations of glutamate and aspartate in rat hippocampus during transient cerebral ischemia monitored by intracerebral microdialysis. J. Neurochem. 43, 1369–1374.

Betz, A.L., Yang, G.Y., Davidson, B.L., 1995. Attenuation of stroke size in rats using an adenoviral vector to induce overexpression of interleukin-1 receptor antagonist in brain. J. Cereb. Blood Flow Metab. 15, 547–551.

Busto, R., Dietrich, W.D., Globus, M.Y.-T., Valdés, I., Sheinberg, P., Ginsberg, M.D., 1987. Small differences in intra-ischemic brain temperature critically determine the extent of ischemic neuronal injury. J. Cereb. Blood Flow Metab. 7, 729–738.

Christenson, S.D., Lake, K.D., Ooboshi, H., Faraci, F.M., Davidson, B.L., Heistad, D.D., 1998. Adenovirus-mediated gene transfer in vivo to cerebral blood vessels and perivascular tissue in mice. Stroke 29, 1411–1416.

Futrell, N., Garcia, J.H., Peterson, E., Millikan, C., 1991. Embolic stroke in aged rats. Stroke 22, 1582–1591.

Globus, M.Y.-T., Busto, R., Martinez, E., Valdés, I., Dietrich, W.D., Ginsberg, M.D., 1991. Comparative effect of transient global ischemia on extracellular levels of glutamate, glycine, and (γ-aminobutyric acid in vulnerable and nonvulnerable brain regions in the rat. J. Neurochem. 57, 470–478.

Hayashi, K., Morishita, R., Nakagami, H., Yoshimura, S., Hara, A., Matsumoto, K., Nakamura, T., Ogihara, T., Kaneda, Y., Sakai, N., 2001. Gene therapy for preventing neruonal death using hepatocyte growth factor: in vivo gene transfer of HGF to subarachnoid space prevents delayed neuronal death in gerbil hippocampal CA1 neurons. Gene Ther. 8, 1167–1173.

Heistad, D.D., Faraci, F.M., 1996. Gene therapy for cerebral vascular disease. Stroke 27, 1688–1693.

Isner, J.M., 2002. Myocardial gene therapy. Nature 415, 234–239.

Isner, J.M., Vale, P.R., Symes, J.F., Losordo, D.W., 2001. Assessment of risks associated with cardiovascular gene therapy in human subjects. Circ. Res. 89, 389–400.

Kirino, T., 1982. Delayed neuronal death in the gerbil following ischemia. Brain Res. 239, 57–69.

Khurana, V.G., Smith, L.A., Baker, T.A., Eguchi, D., O'Brien, T., Katusic, Z.S., 2002. Protective vasomotor effects of in vivo recombinant endothelial nitric oxide synthase gene expression in a canine model of cerebral vasospasm. Stroke 33, 782–789.

Kitagawa, H., Sasaki, C., Sakai, K., Mori, A., Mitsumoto, Y., Mori, T., Fukuchi, Y., Setoguchi, Y., Abe, K., 1999. Adenovirus-mediated gene transfer of glial cell line-derived neurotrophic factor prevents ischemic brain injury after transient middle cerebral artery occlusion in rats. J. Cereb. Blood Flow Metab. 19, 1336–1344.

Lawrence, M.S., Sun, G.G., Kunis, D.M., Saydam, T.C., Dash, R., Ho, D.Y., Sapolsky, R.M., Steinberg, G.K., 1996. Overexpression of the glucose transporter gene with a herpes simplex viral vector protects striatal neurons against stroke. J. Cereb. Blood Flow Metab. 16, 181–185.

Linnik, M.D., Zahos, P., Geschwind, M.D., Federoff, H.J., 1995. Expression of bcl-2 from a defective herpes simplex virus-1 vector limits neuronal death in focal cerebral ischemia. Stroke 26,1670–1674.

Mies, G., Kohno, K., Hossmann, K.A., 1993. MK-801, a glutamate antagonist, lowers flow threshold for inhibition of protein synthesis after middle cerebral artery occlusion of rat. Neurosci. Lett. 155, 65–68.

Millikan, C., 1992. Animal stroke model. Stroke 23, 795–797.

Minamisawa, H., Smith, M.L., Siesjö, B.K., 1990. The effect of mild hypothermia and hypothermia on brain damage following 5 10, and 15 minutes of forebrain ischemia. Ann. Neurol. 28, 26–33.

Muhonen, M.G., Ooboshi, H., Welsh, M.J., Davidson, B.L., Heistad, D.D., 1997. Gene transfer to cerebral blood vessels after subarachnoid hemorrhage. Stroke 28, 822–829.

Nabel, E.G., Plautz, G., Nabel, G.J., 1990. Site-specific gene expression in vivo by direct gene transfer into the arterial wall. Science 249, 1285–1288.

Ono, S., Date, I., Onoda, K., Shiota, T., Ohmoto, T., Ninomiya, Y., Asari, S., Morishita, R., 1998. Decoy administration of NF-kappaB into the subarachnoid space for cerebral angiopathy. Hum. Gene Ther. 9, 1003–1011.

Ooboshi, H., Sadoshima, S., Yao, H., Ibayashi, S., Matsumoto, T., Uchimura, H., Fujishima, M., 1995a. Ischemia-induced release of amino acids in the hippocampus of aged hypertensive rats. J. Cereb. Blood Flow Metab. 15, 227–234.

Ooboshi, H., Welsh, M.J., Rios, C.D., Davidson, B.L., Heistad, D.D., 1995b. Adenovirus-mediated gene transfer in vivo to cerebral blood vessels and perivascular tissue. Circ. Res. 77, 7–13.

Ooboshi, H., Rios, C.D., Chu, Y., Christenson, S.D., Faraci, F.M., Davidson, B.L., Heistad, D.D., 1997a. Augmented adenovirus-mediated gene transfer to atherosclerotic vessels. Arterioscler. Thromb. Vasc. Biol. 17, 1786–1792.

Ooboshi, H., Rios, C.D., Chu, Y., Faraci, F.M., Davidson, B.L., Heistad, D.D., 1997b. Altered vascular function following adenovirus-mediated overexpression of endothelial nitric oxide synthase. Am. J. Physiol. 273, H265–H270.

Ooboshi, H., Rios, C.D., Heistad, D.D., 1997c. Novel methods for adenovirus-mediated gene transfer to blood vessels in vivo. Mol. Cell. Biochem. 172, 37–46.

Ooboshi, H., Toyoda, K., Faraci, F.M., Lang, M.G., Heistad, D.D., 1998. Improvement of relaxation in an atherosclerotic artery by gene transfer of endothelial nitric oxide synthase. Arterioscler. Thromb. Vasc. Biol. 18, 1752–1758.

Ooboshi, H., Ibayashi, S., Takada, J., Yao, H., Kitazono, T., Fujishima, M., 2001. Adenovirus-mediated gene transfer to ischemic brain. Ischemic flow threshold for transgene expression. Stroke 32, 1043–1047.

Pang, L., Ye, W., Che, X.M., Roessler, B.J., Betz, A.L., Yang, G.Y., 2001. Reduction of inflammatory response in the mouse brain with adenoviral-mediated transforming growth factor-ss1 expression. Stroke 32, 544–552.

Pulsinelli, W.A., Brierley, J.B., Plum, F., 1982. Temporal profile of neuronal damage in a model of transient forebrain ischemia. Ann. Neurol. 11, 491–498.

Rios, C.D., Ooboshi, H., Piegors, D., Davidson, B.L., Heistad, D.D., 1995. Adenovirus-mediated gene transfer to normal and atherosclerotic arteries. A novel approach. Arterioscler. Thromb. Vasc. Biol. 15, 2241–2245.

Schneider, M.D., French, B.A., 1993. The advent of adenovirus. Gene therapy for cardiovascular disease. Circulation 88, 1937–1942.

Shimazaki, K., Urabe, M., Monahan, J., Ozawa, K., Kawai, N., 2000. Adeno-associated virus vector-mediated bcl-2 gene transfer into post-ischemic gerbil brain in vivo: prospects for gene therapy of ischemia-induced neuronal death. Gene Ther 7, 1244–1249.

Shurr, A., Tseng, M.T., West, C.A., Rigor, B.M., 1987. Taurine improves the recovery of neuronal function following cerebral hypoxia: an in vitro study. Life Sci. 40, 2059–2066.

Toyoda, K., Ooboshi, H., Chu, Y., Fasbender, A.J., Faraci, F.M., Davidson, B.L., Heistad, D.D., 1998. Cationic molecules enhance adenovirus-mediated gene transfer to the carotid artery. Stroke 29, 2181–2187.

Toyoda, K., Faraci, F.M., Watanabe, Y., Ueda, T., Andresen, J.J., Chu, Y., Otake, S., Heistad, D.D., 2000. Gene transfer of calcitonin gene-related peptide prevents vasoconstriction after subarachnoid hemorrhage. Circ. Res. 87, 818–824.

Trapnell, B.C., 1993. Adenoviral vectors for gene transfer. Adv. Drug Deliv. Rev. 12, 185–199.

Ueda, K., Hasuo, Y., Ohmura, T., Kiyohara, Y., Kawano, H., Kato, I., Shinkawa, A., Iwamoto, H., Nakayama, K., Omae, T., Fujishima, M., 1990. Causes of death in the elderly and their changing pattern in Hisayama, a Japanese community. Results from a long-term and autopsy-based study. J. Am. Geriatr. Soc. 38, 1332–1338.

Ueda, K., Kawano, H., Hasuo, Y., Fujishima, M., 1992. Prevalence and etiology of dementia in a Japanese community. Stroke 23, 798–803.

Verma, I.M., Somia, N., 1997. Gene therapy—promises, problems and prospects. Nature 389, 239–242.

Watanabe, Y., Chu, Y., Andresen, J.J., Nakane, H., Faraci, F.M., Heistad, D.D., 2002. Gene transfer of extracellular superoxide dismutase reduces vasospasm following subarachnoid hemorrhage. Stroke 33, 375.

Wolf, P.A., Kannel, W.B., D'Agostino, R.B., 1998. In: Ginsberg, M.D., Bogousslavsky, J. (Eds.), Epidemiology of Stroke, Cerebrovascular Disease: Pathophysiology, Diagnosis, and Management, Blackwell Science, Malden, pp. 834–849.

Xie, Y., Mies, G., Hossmann, K.A., 1989. Ischemic threshold of brain protein synthesis after unilateral carotid artery occlusion in gerbils. Stroke 20, 620–626.

Xu, D.G., Crocker, S.J., Doucet, J.P., St-Jean, M., Tamai, K., Hakim, A.M., Ikeda, J.E., Liston, P., Thompson, C.S., Korneluk, R.G., MacKenzi, A., Robertson, G.S., 1997. Elevation of neuronal expression of NAIP reduces ischemic damage in the rat hippocampus. Nat. Med. 3, 997–1004.

Yagi, T., Jikihara, I., Fukumura, M., Watabe, K., Ohashi, T., Eto, Y., Hara, M., Maeda, M., 2000. Rescue of ischemic brain injury by adenoviral gene transfer of glial cell line-derived neurotrophic factor after transient global ischemia in gerbils. Brain Res. 885, 273–282.

Yang, G.Y., Mao, Y., Zhou, L.F., Gong, C., Ge, H.L., Betz, A.L., 1999. Expression of intercellular adhesion molecule 1(ICAM-1) is reduced in permanent focal cerebral ischemic mouse brain using an adenoviral vector to induce overexpression of interleukin-1 receptor antagonist. Mol. Brain Res. 65, 143–150.

Yang, G.Y., Pang, L., Ge, H.L., Tan, M., Ye, W., Liu, X.H., Huang, F.P., Wu, D.C., Che, X.M., Song, Y., Wen, R., Sun, Y., 2001. Attenuation of ischemia-induced mouse brain injury by SAG, a redox-inducible antioxidant protein. J. Cereb. Blood Flow Metab. 21, 722–733.

Yao, H., Sadoshima, S., Ooboshi, H., Sato, Y., Uchimura, H., Fujishima, M., 1991. Age-related vulnerability to cerebral ischemia in spontaneously hypertensive rats. Stroke 22, 1414–1418.

Yao, H., Ooboshi, H., Ibayashi, S., Uchimura, H., Fujishima, M., 1993. Cerebral blood flow and ischemia-induced neurotransmitter release in the striatum of aged spontaneously hypertensive rats. Stroke 24, 577–580.